Robotic Wheelchair for Navigating Urban Environments

(都市環境を走行するロボット車いす)

2018 年 9 月

埼玉大学大学院理工学研究科（博士後期課程）

理工学専攻 (主指導教員　久野　義徳)

SHAMIM AL MAMUN
（シャーミム アロ マムン）

Robotic Wheelchair for Navigating Urban Environments

SHAMIM AL MAMUN
Graduate School of Science and Engineering
Saitama University, JAPAN
Supervisor: Professor Yoshinori Kuno

A thesis submitted in partial fulfillment of the requirementfor the degree of

Doctor of Philosophy

September, 2018

To my late Father and late elder brother

Mohammad Abdul Bari

Md. Abul Kalam Azad

Acknowledgements

First of all, I thank ALLAH for giving me the strength and ability to complete this study. There are also many people who have supported and encouraged me throughout this doctoral research that I would like to acknowledge.

I would like to thank my supervisor ***Professor Yoshinori Kuno***, Saitama University, Japan, for his trust, continuous support, guidance, and patience over the past few years. I am sincerely grateful to him for his constant encouragement, and his stimulating ideas.

I am incredibly grateful to ***Professor Yoshinori Kobayashi, and Assistant Professors Antony Lam and Hisato Fukuda*** for their comments, insightful discussions, valuable advice, and feedback during evaluating of my thesis work. I am forever thankful to ***Dr. Ryota Suzuku*** for the valuable time that you have given to me.

Finally my friends, colleagues and relatives for their continuous encouragement in my hectic time of research work. And very certainly not least, I am grateful to my son ***Roudroneel Mamun*** and my wife ***Suhana Parvin*** who had to bear with my moods and impatience whenever the research did not work out the way I wanted. There are too people that have helped me while staying abroad to name personally, but I am sure you know who you are. Thank you, and thank you all for your kind support and encouragement.

Abstract

In the last decade, several robotic wheelchairs possessing user-friendly interfaces and/or autonomous functions for reaching goals have been proposed to meet the needs of an aging society. The elderly and disabled currently use different kinds of wheelchairs that are either manually controlled or powered by a control system. Although wheelchairs make it possible, for their users to go out alone, users are in practice often accompanied by companions such as friends, families and caregivers. The workload of assistive companions can be reduced with the help of motorized wheelchairs. However, even motorized wheelchairs have some shortcomings and discouraged by some doctors, especially in cases where the elderly need to navigate urban environments and perform tasks such as boarding buses or climbing up a certain height. Thus, in designing new wheelchair technologies, it is important to consider how we can reduce the caregivers workload while overcoming the existing shortcomings of wheelchairs. Autonomous wheelchairs are a potential solution to these issues, which could also have the option of granting many elderly wheelchair users the ability to control their wheelchairs on their own. In fact, this thesis reviewed that around 3 million people could benefit from such wheelchairs. However the large majority of research to date has focused on indoor navigation. Thus, this thesis is specifically concerned with navigation in outdoor urban environments while considering practical issues such as the cost of sensors and the computational cost of the robotic wheelchair. More specifically, this thesis is aimed at first developing and designing a sensing system which can detect conditions in outdoor terrain for the wheelchair to run smoothly. The thesis then focuses on getting precise measurements using a bidirectional sensing system with a single 2D laser for boarding and disembarking buses autonomously in urban environments. The empirical part of this thesis was conducted throughout the study period and involved developing an autonomous bus boarding wheelchair system that moves independently with a companion or caregiver in urban terrain to

reach bus stations and the wheelchair also has the capability to find bus doors using precise measurements and then boards using mechanically adjusted wheels.

To achieve these goals, the thesis first proposes a robotic wheelchair system that is able to classify the type of outdoor terrain according to their roughness for the comfort of the user and also control the wheelchair movements to avoid step edges and watery areas on the road. The thesis study found that the wheelchairs terrain surfaces can be classified into four different categories. These are rough surfaces, watery places on the road, indoor plain surfaces, and dirt tracks. These roads may have different conditions, which can be dangerous for the wheelchair user due to the risk of sudden accidents when driving over them. Suppose a wheelchair follows the caregiver but s/he misses hazards such as bumpy/pit areas or watery spots. If the wheelchair were to not actively look for such hazards, it could fall and lead to injury of the occupant. Moreover, the wheelchairs speed for different surface areas should not be same. The wheelchairs speed need to be automatically controlled with care. For this reason, detecting the type of surface is a necessity. An artificial neural network based classifier was constructed to classify the patterns and features extracted from the Laser Range Sensor (LRS) intensity and distance data. The overall classification accuracy was found to be 97.24% using extracted features from the intensity and distance data. These classification results can in turn be used to control the motor of the smart wheelchair. Moreover, the computed 3D surface elevation map could be used for making the decision of whether to move-on, slow down the speed, or to avoid watery and muddy areas on the road. Finally, this classification method was implemented on the wheelchair to validate its effectiveness by an experiment in which the proposed wheelchair system could detect watery places on the road and avoid them in a very efficient manner.
Classification of terrain is not all about smooth navigation where smart wheelchair systems aim to reduce the workload of the caregiver. In this thesis, a novel 3D sensing system is introduced. It consists of a triangular shaped apparatus with undistorted reflecting mirrors for vertical and horizontal sensing of the floor with a conventional single 2D Laser range

sensor and we name it Bidirectional sensing system (BSS). Conventionally 2D laser sensors have a wide-angle horizontal field of view. We use a 2D LRF (HOKUYO) that has a horizontal angle view field of 270°, with a measuring interval angle of 0.25°. Typically, researchers uses two or more such laser sensors to obtain vertical and horizontal sensing points for measurement of heights. However, a single scan from the LRF captures 1080 values in 25 ms, representing a viewing angle of 270° but we do not need to scan all 270° in the horizontal field of view. On the other hand, we do need some vertical scan data to detect steps. Thus, we divided the total view angle into three parts with a 90° view angle each by using three undistorted reflecting mirrors. All acquired data from the 2D laser had outliers removed so that we could accurately measure the step size of stairs or the elevation gaps of bus doors. In order to remove any undesirable artifacts, we use the median values and standard deviation of the data series. Deploying our BSS titled towards the ground at 45° and 100 cm above, the slope was calculated from the laser data to find whether it was positive or negative. A positive tangent indicates a planar surface and a negative slope indicates steps. In our system, the scanning points are separated in such way that they give two horizontal scanning lines and one vertical scanning line. For the vertical positional data, we get distributions for every step of a given height like in the case of stairs or the doorstep of a bus in the $y - direction$ and the $z - direction$. Here, y and z indicate the horizontal and vertical spaces of the data plot respectively. The $z - values$ give the height whereas the $y - values$ give the width, respectively. The standard deviation and mean of each direction are used for finding outliers. Then the mode of the distribution of the values are applied to find the peak points and lowest point. The Euclidian distance of those, two points are then used to determine the height of the steps. For finding the mode, we used 1 cm intervals in each direction. Therefore, this sensing system is able to calculate precise measurements of bus doorsteps or staircase steps for climbing. For measuring the accuracy of this sensing system, we calculated stair and bus doorstep heights in practical scenarios and were able to measure heights with an error of $\pm 1cm$.

Finally, the major objective of this thesis is to build an autonomous

wheelchair to board buses. For bus boarding, we need two vertical scanning lines set apart at a distance the same as the wheelchair width so that it can avoid collisions with the bus door. Therefore, we used two BSSs and a calibrated camera equipped along the same axis on a 78 cm long bar edge tilted to the ground. This gives two vertical sensing lines from the far left and right of the sensors and four horizontal sensing lines across the vertical lines. Theoretically, we merge the horizontal data from the top and bottom so that we can receive a single distance value from both sensors. Additionally, we mapped these 3D point cloud data onto an image for verification and experimentation. The vertical sensing positions of the sensors start from 3 cm by the front wheels to check for obstacles. Our sensing area also covers 1 meter of the distance ahead of wheelchair. The front area of the sensing lines are important to find other obstacles like other passengers, bus seats, or luggage. Once the wheelchair has been instructed to board the bus, our system can sense if this area is free to board, otherwise it sets itself back. This feature adds an extra layer of safety for our wheelchair. Also, before receiving any bus boarding commands, our wheelchair is able to detect the bus door using an image recognition system. For that, the YOLO Darknet based object detection approach is employed. For approximate detection of buses and bus doors with doorsteps, we trained our image recognition system with 400 different images of buses, bus doors and doorstep for each class. In addition, the overall precision of the system was measured using the Intersection of Union (IoU) method and we achieved an overall 88% average. In a real experiments with a buses, we see the effectiveness in detecting the buses and bus doors. Our wheelchair also approached to a bus and measured the doorstep height to be 14.9 cm where the actual height was measured to be 15 cm.

In addition, we made our wheelchair capable of autonomously following its companion on way to the bus station for smooth running on terrain and then had it wait for the bus. In our setup, once our image recognition system detects the bus, it changes its position to move to the approximate location of the door. Once the door is detected, the wheelchair guided by the BSS module to find the bus doorsteps and calculates the height and width of the door for boarding. To achieve these tasks, our wheelchair operates in three modes (1) Companion Following Mode, (2)

Autonomous Mode for boarding and (3) Manual Mode. The companion following mode is in operation while the wheelchair is going to the bus stop and after getting off from the bus. The autonomous mode is operated while the wheelchair is either boarding or getting off the bus. As space is limited inside the bus, the wheelchair is operated in manual mode with a joystick by the companion for adjusting the wheelchair position towards the bus door for safe navigation. We conducted several indoor mock-up bus experiments and real bus experiments for bus boarding with a newly trained image recognition server that can detect buses and bus doors as well as doorsteps. Based on the experimental results of this research, it can be concluded that a new mechanism of bidirectional sensing using a single 2D laser for getting the heights of bus doorsteps for autonomous bus boarding was successful. Moreover, we demonstrated successfully operation of the proposed robotic wheelchair system using our method, which grants freedom of movement to the wheelchair user in urban environments.

Contents

1 Introduction **1**

1.1 Motivation 1

1.2 Objectives 4

1.3 Research Contribution 5

1.4 Organization of Sections 6

2 Interdisciplinary Background **8**

2.1 Review of Robotic Wheelchairs 8

2.1.1 Robotic Wheelchair 8

2.2 Robotic Wheelchair Hardware 10

2.2.1 Sensors 10

2.2.2 Conventional 2D Laser Range Sensor 12

2.3 Mobility Functionality of Robotic Wheelchair 14

2.4 Chapter Summary 15

3 Terrain Recognition **16**

3.1 Introduction 16

3.2 Surface Classification Methodology 18

3.2.1 Conditioning of Raw LRS data 19

3.2.2 Segmentation and Windowing 21

3.2.3 Surface 3D Map Generation 21

3.2.4 Feature Extraction 22

3.2.5 Classification Model 23

3.3 Experiment and Results 24

3.4 Chapter Summery 27

4 Single Laser Bidirectional Sensing **28**
4.1 Introduction and Motivation 28
4.2 Robotic Wheelchair System 30
4.3 Data Acquisition Method 31
4.3.1 2D Sensor Using Undistorted Mirrors 32
4.3.2 Coordinate Transformation from Laser Data to Camera Image Plane 33
4.3.3 Positioning the Laser Data onto the Camera Image Plane . . . 35
4.4 Step Measuring Methodology 36
4.5 Experiment Result 37
4.5.1 Upward Stair Measurement 37
4.5.2 Bus Floor 38
4.6 Chapter Summery 40

5 Bus Boarding Wheelchair and Autonomous Companion Following Mode **41**
5.1 Introduction 41
5.2 System Overview 43
5.2.1 BMR Hardware 43
5.2.2 Detection Software 45
5.3 Bus, Bus door and doorsteps Detection 45
5.4 Bidirectional Sensing System (BSS) 49
5.4.1 Sensor System 49
5.4.2 Mapping Sensor Data on Camera Image 52
5.5 Experimental Setup 53
5.5.1 Step Detection and Position Correction 54
5.5.2 BMR Control 54
5.6 Experiment Results 55
5.7 Moving Alongside Companion 57
5.8 Adjust Wheelchair Position 64
5.9 Chapter Summary 67

6 Conclusions and Future Works **68**
6.1 Conclusions 68
6.2 Future Work 69

Bibliography **71**

List of Figures

1.1 Bus Boarding Robotic Wheelchair in Real Bus Experiment Setup . . 3
1.2 Bidirectional sensing system for robotic wheelchair 5

2.1 Examples of modern PW form factors: (a) Stair climbing iBot [51], (b) Australia's Ability in Motion [20], standing wheelchair, (c) the Tank Chair [4], (d) Chinese Observer remains level on all-terrain [66], and (e) Patrafour by Toyota Motor East Japan [24]. 9
2.2 Conventional Laser Sensors 12
2.3 Different types of sensors used in smart or robotic wheelchairs. 13
2.4 HOKUYO UST 10LX 13
2.5 Sample output from 2D laser range sensor. 13

3.1 General block diagram of the whole procedure. 18
3.2 Arrangement of laser for surface roughness data calculation. 19
3.3 Proposed wheelchair system. 20
3.4 Data data collection apparatus. 20
3.5 3D elevation map from surface patches: (a) Asphalt road, (b) Dirt track, (c) Indoor, and (d) Watery places. 22
3.6 Structure of adaptive neuro-fuzzy inference system using neuro-Fuzzy Designer in Matlab with 3 inputs and one output. 24
3.7 Example scene of data collection sites: (a) Indoor (b) Dirt track (c) walkway (d) watery places on the road after rain. 25

4.1 Robotic Wheelchair 31
4.2 Schematic diagram of wheelchair wheel positions for boarding a bus. . 32
4.3 Schematic Diagram of Our Sensing System. 33
4.4 Sensing apparatus using HOKUYO UTM-30LX with reflecting mirror. 34
4.5 Schematic flowchart of laser data mapping on to the image. 35
4.6 Real time fusion results from video images. 36
4.7 Methodology of finding the step size of bus and stairs. 36

4.8 Methodology of finding the step size of the bus or stair. 39

5.1 Bus boarding robotic wheelchair with new sensing mechanism. 42
5.2 Hardware of Smart Wheelchair System 44
5.3 System Flowchart 47
5.4 Different Types of Bus Detections Using SSD 48
5.5 Image Detection Using SSD 48
5.6 Open and Closed Door Detection 49
5.7 Bidirectional Sensing System (BSS) 50
5.8 3D Projection of Sensor Data 51
5.9 Mock-up Bus for Indoor Experiments 53
5.10 Visual camera images for boarding: (a) Running State (b) Detected bus doorstep (c) Adjusting its distance for safe boarding (d) Boarding 56
5.11 Our Wheelchair System Autonomously Boarding the Bus 57
5.12 Real bus boarding experiment 58
5.13 Real bus disembarking experiment 59
5.14 Contour observation model and likelihood evaluation by the laser. . . 60
5.15 Trajectories of BMR and Companion 61
5.16 Apparatus of companion following. 62
5.17 Apparatus of companion following. 62
5.18 Tracking the companion in three different zones. 63
5.19 The wheelchair is navigating according to the body orientation and position. 64
5.20 Laser scanner data position on bus body. 65
5.21 Laser scanner data position on bus body. 66

List of Tables

2.1 Categories of wheelchairs according to the past, present and future) . 10
2.2 Hardware summary of the robotic wheelchair) 12

3.1 Feature values of different types of surface data (intensity values) . . 23
3.2 Confusion matrix for the pattern classification method (4 classes for each test surface). 26

4.1 Measurement of the steps (in cm) and error percentage. 38

Chapter 1

Introduction

1.1 Motivation

In the last decade, people with cognitive/motor/sensory impairment, whether it is due to disability or disease or aging, rely on power wheelchairs for their mobility needs. Since some people with disabilities cannot use a traditional joystick to navigate their powered wheelchair (PW), they use alternative control systems like head joysticks, chin joysticks, sip-n-puff, and thought control [38][48][8][64][7]. In many cases, PW users have difficulties with daily maneuvering tasks and would benefit from an automated navigation system. Mobility aside, people with disabilities are heavily reliant on their caregivers for eating and drinking, handling items, and communicating with others, especially in large groups. To accommodate the population of individuals who find it difficult or impossible to operate a PW, several researchers have used technologies originally developed for mobile robots to create smart wheelchairs (SWs) [64][53][72][30][23]. An SW typically consists of either a standard PW base to which a computer and a collection of sensors have been added, or a mobile robot base to which a seat has been attached [63]. Pineau et al. argue that the transition to wheelchairs that cooperate with the user is at least as important as that from manual to powered wheelchairs, possibly even more important since this would mark a paradigmatic rather than merely a technological shift [49].

While alternatives to joystick mediums enable the target patient to maneuver, the navigation burden is still totally on the user. According to [55], among 200 practicing clinicians in the U.S., 40% of their patients find it hard or impossible to control the wheelchair even with such alternative mediums. Most recently, it has also been reported in [10] that most patients with motor impairments are unable to steer the wheelchair for avoiding obstacles and parallel parking. These clinical findings provide insight for the importance for devising a computer-controlled platform to assist the

users by reducing their workload and increasing safety. In this framework, user input along with environmental information will be seamlessly analyzed for performing necessary assistive tasks. The amount of given assistance usually varies depending on how severe the users' impairments. The assistance can be categorized into three main levels; shared-control, semiautonomous control, and autonomous control [68]. The level of given assistance should be decided by considering the maximum of users abilities to control the wheelchair first, and the computer will complement the holes in ability [19]. Shared control lets the user fully command the wheelchair. The computer only steps in when it is absolutely necessary (e.g. passing through a door or avoiding obstacles) [3]. Autonomous control lets the wheelchair move automatically on routes to the final destination pre-selected by the user [31]. Due to such nature, shared-control is more suitable to the users who can provide continuous input command with a joystick. Autonomous control is more adequate to the users who are unable to provide low level orders, who feel fatigue easily, and who have visual impairment [5]. Since people with severe motor disabilities can still command their heads even with limited amount of movement, semi-autonomous control is a proper assistive choice. In this control mode, the computer performs short-term route planning, and the users only intervenes when they wish to deviate from the plan [46]. This means that, once a command is issued, the users can relax while the computer is completing the task. Unlike in autonomous control, semi-autonomous control does not need an actual map of the environment; only a local safety map based on sensor scans is needed. Hence it can give freedom to the users to move in new environments.

Moreover in recent years, millions of people around the world have exhibited mobility impairments due to aging problems. Thus the development of powered wheelchairs that can overcome doctors' safety concerns would be of great benefit to many. In fact, [28] found that around three million people could benefit from such wheelchairs. But the main goal of researchers are user-friendly interfaces or the autonomous behavior of wheelchairs for moving toward some goal like a shopping mall, train station, or bus stop while avoiding obstacles in the terrain [40],[27],[36]. Although it is often desirable for users to operate wheelchairs on their own, they are often accompanied by a caregiver or companion. Therefore, researchers want an autonomous wheelchair, which can reduce the workload for the companion to lead the wheelchair users using tools such as a remote controller or lifting the wheelchair to overcome some heights on the road or getting on stairs or ramps [21],[57]. Moreover, [58] proposed an SWS ecosystem that has two primary components: a mapping service which generates large-scale landmark maps, and the SWS vehicle itself, which is a client of the mapping service

using 3D LIDAR imaging system to provide a robust perception in unstructured outdoor environments. In addition, object recognition is a challenging part to detect objects in real time with labeling on the image frame. Therefore, researchers are using different types of sensors to accumulate the environmental information. Regarding this, we note that semantic segmentation [67] of the image is very helpful for our purposes. In particular, semantic segmentation approaches [9] yield good solutions for object detection using a variation of Convolutional Neural Networks in which a new def-pooling layer and learning strategies such as in Region-based Convolutional Neural Networks or Deep Belief Networks are employed. Great strides have been made in recent years but processing speed still presents challenges to applications in realtime systems. That is why some researchers have proposed regression models [54] for deep learning to speed up processing time such as with YOLO and SSD. The authors of those papers proposed that they discretize the output space of the bounding boxes into a set of default boxes over different aspect ratios and scales per feature map location. At prediction time, the network generates scores for the presence of each object category in each default box and produces adjustments to the box to better match the object shape. Moreover, they frame object detection as a regression problem to spatially separated bounding boxes and associated class probabilities. And they showed that their system runs at 59-67 FPS with mAP 76.85, which outperforms with other detection methods.

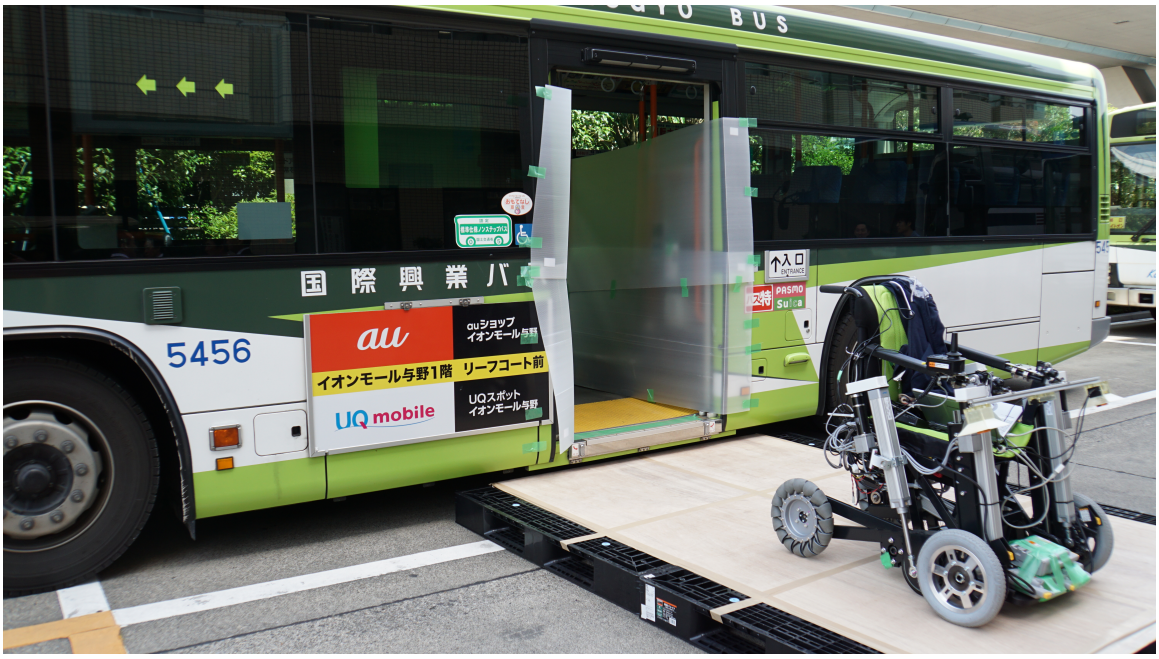

Figure 1.1: Bus Boarding Robotic Wheelchair in Real Bus Experiment Setup

1.2 Objectives

Therefore, a new mechanism for a robotic wheelchair is needed that can detect steps and have the capability to move onto bus doorsteps or climb onto stairs. For bus boarding, wheelchairs need 3D measurements to get precise measurements of the doorstep's height and door width. Vision based systems can be a good option for this kind of information [33]. A 3D depth camera can also be used for terrain mapping with depth information. But for outdoor applications, saturation issues may occur due to sunlight. Moreover, the computational cost can be too high for real time applications in bus boarding robotic wheelchairs and the measurements may be inaccurate. For precise movement of the smart wheelchair, it is very important to identify the observable area ahead of the wheelchair with faster detection tools. However, we note that most robotic wheelchairs use one or more 2D laser devices to avoid hazards like narrow passes, slopes, and stairs [43]. In particular, much of the previous work concerns the use of 2D Laser Range Finder (LRF) sensors for obstacle detection. However, using multiple sensors or any moving mechanism for sensing results in a more complex system, thus increasing computational cost and the need for maintenance. Although, instead of using 3D sensors, in [1] the authors presented some 3D sensing systems using 2D LRFs. In those systems, multiple LRF sensors installed in different directions were mounted on a rotating unit to sense environmental hazards or for terrain classification. Fujita and Kondo [70] developed a sensing system using an arm-type sensor movable unit, which can sense in horizontal and vertical spaces to model stairs and gaps. The authors showed that their robot could measure the step size of stairs fairly well. Likewise, they had a 5.8% error in calculating the step height and width.

Therefore, we propose our own approach to outdoor navigation with autonomous functionalities. While we are also concerned with dynamic obstacles, the emphasis of this thesis is in developing a sensor framework (see Fig. 1.2 where bidirectional sensing is required to measure height and width with a single 2D laser sensor) that can classify the terrain according to smoothness like indoor, outdoor road, muddy places or side walk, and watery areas to avoid. Then our wheelchair follows its companion autonomously to reduce the physical load for stepping onto buses or disembarking from buses.

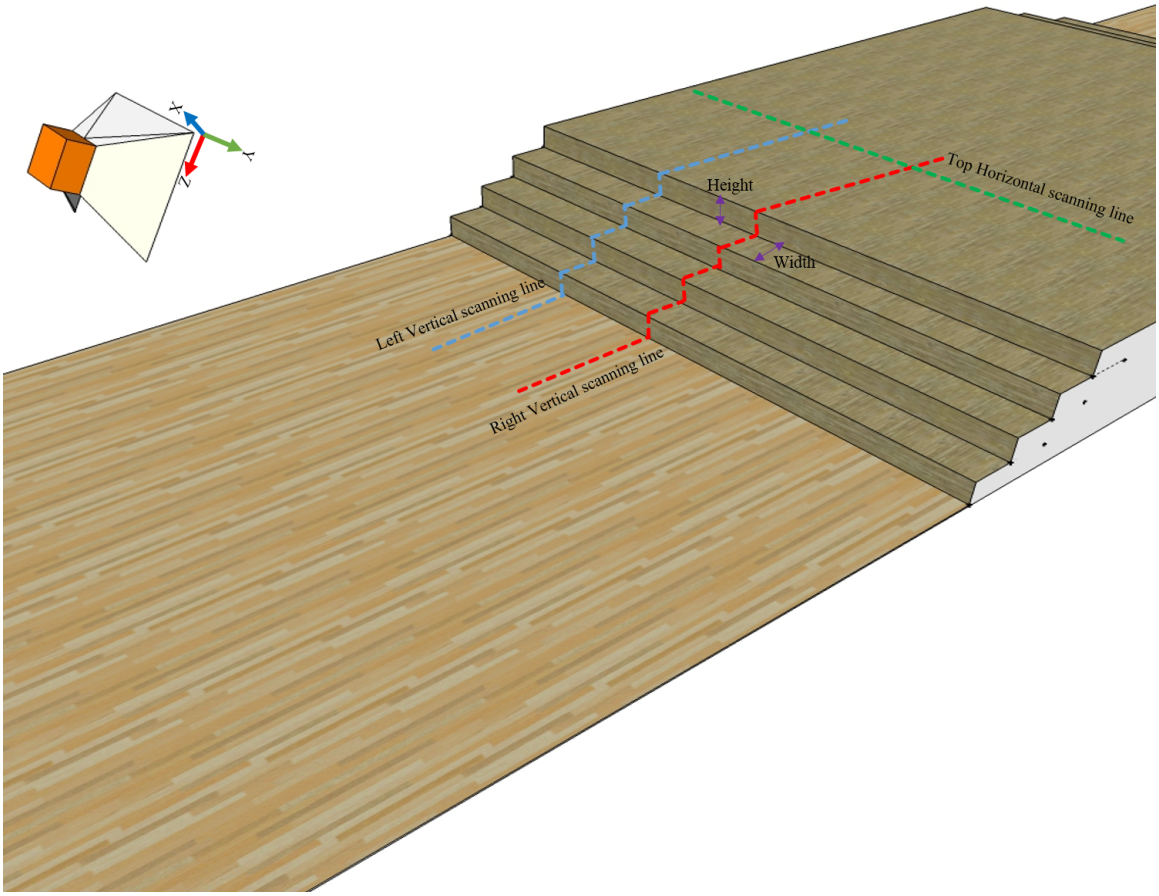

Figure 1.2: Bidirectional sensing system for robotic wheelchair

1.3 Research Contribution

This research result in designing bus boarding autonomous mobility robot wheelchair with a novel sensing framework to scan road condition with classification for recognizing terrain. Moreover, for safe and comfortable navigation, it should has the capability to follow its companion to get onto the bus.

- An experimental paradigm for studying how robotic wheelchairs can identify the terrain and its condition while it is out with its companion or caregiver (Chapter 3).
- An experimental paradigm for studying how a sensing system is used for classification and the way to use it (Chapter 3).
- An experimental paradigm for studying how to design a new sensing framework that can act as 3D sensor with a single laser sensor (Chapter 4).

- An experimental paradigm for studying how to measure the height of the obstacle and determine whether to climb onto it or not (Chapter 4).
- An experimental paradigm for designing a new mechanism for boarding on a bus (Chapter 5).
- An experimental paradigm for describing how the autonomous wheelchair follows its companion and find a bus and bus door with its precise measurement of the door for boarding (Chapter 5).
- Finally, an experimental paradigm for designing the operating mode to follow its companion on the way to bus stop and embarking and disembarking from buses with safety measurements (Chapter 5).

1.4 Organization of Sections

Chapter 2 - Interdisciplinary Background

This chapter provides the interdisciplinary background and current state-of-art to the different topics treated in this thesis.

Chapter 3 - Terrain Recognition

In Chapter 3, a NeuroFuzzy based classification technique is applied for recognition of different kinds of terrain so that the robotic wheelchair can choose the right path and avoid hazards on road to navigate itself safely. The chapter also explains the results of experiments conducted in real scenarios based on statistical and empirical methods.

Chapter 4 - Single Laser Bidirectional Sensing

A conventional 2D laser device is used for measuring height and width. We show that a single 2D laser device can be used as a 3D measuring device. Therefore, a novel technique is described in this chapter to measure the height and width of an object so that the wheelchair can overcome heights without any collisions.

Chapter 5 - Bus Boarding Wheelchair and Autonomous companion Following Mode

In this chapter, robotic wheelchair experimental data is shown using new framework of sensing 3D measurement. Object recognition is also described at the end of this chapter with its accuracy which is used for the bus boarding robotic wheelchair with companion following mode.

Chapter 6 - Conclusions

We conclude the thesis with a summary of the concepts and designed sensor framework which can be adopt in wheelchairs to make it more convenient to measure the height of an object to climb onto it followed by the potential future works and applications.

Chapter 2

Interdisciplinary Background

We review the concepts and showcase the latest human-computer interface hardware, sensor processing algorithms, and machine-vision innovations made in recent years. These tools give people with disabilities not only mobility but also the necessary help and support to handle daily living activities. We hope that the information gathered in this study will enhance awareness of the status of contemporary Robotic wheelchair (RW) technology and ultimately increase the functional mobility and productivity of people who use powered wheelchairs (PWs). The rest of this chapter is organized to describe the robotic wheelchairs with their hardware and functionalities.

2.1 Review of Robotic Wheelchairs

2.1.1 Robotic Wheelchair

George Klein invented the first PW for people with quadriplegia injured in World War II, while he was working as a mechanical engineer for the National Research Council of Canada [6]. A person with that level of disability or aging problems is by default bedridden because without assistance from people and/or technology, there would be no way to get up. That being said, with the right combination of human and technological resources, a person with disabilities can still have an extremely rich life and make a major contribution to society, a philosophy we hope to share with people who have just experienced the onset of disability. While primarily intended for people with mobility disabilities, those suffering from ailments resulting in fatigue, and pain can also benefit from a PW. By 1956, Everest and Jennings and the American Wheelchair Company began producing PWs for mass sales [12]. The basic components of a PW are as follows:

- Chassis, or drive system, may be front-wheel, rear-wheel, center-wheel, or all-wheel-drive. Chassis may be foldable [25], include stair-climbing ability (see Fig. 2.1).

- Batteries: The first PWs derived their power from two 24V wet cell batteries. But these batteries have to be removed from the wheelchair during travel on airplanes. They were eventually replaced by dry cell batteries.

- Controller: The interface between human and machine. Commercially available controllers include the hand joystick, sip-n-puff, chin joystick, and head joystick.

- Seating System: Seats are typically upgraded to include cushions that use foam, gel, or air to prevent pressure sores. Backrests are typically padded with foam and can be motorized to tilt and recline. Lateral supports keep the user from tilting side-to-side. Footrests are either removable or motorized to accommodate a more comfortable reclining position.

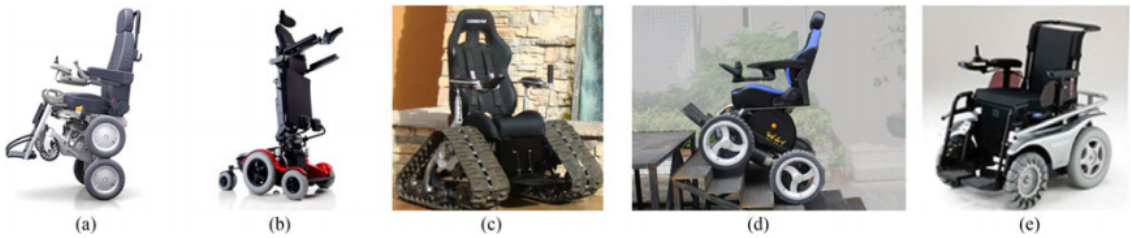

Figure 2.1: Examples of modern PW form factors: (a) Stair climbing iBot [51], (b) Australia's Ability in Motion [20], standing wheelchair, (c) the Tank Chair [4], (d) Chinese Observer remains level on all-terrain [66], and (e) Patrafour by Toyota Motor East Japan [24].

We can categorize all the wheelchairs from the past and present that were guided by human factors to produce the best solutions to current challenges and research on robotic wheelchair features that will be part of future applications as shown in Table 2.1.

Table 2.1: Categories of wheelchairs according to the past, present and future)

Period	Subcategories
Past	Haptic Feedback Voice Recognition Object recognition Human physiology Collision avoidance Social issues
Present	Cloud computing Computer vision Game controller Touch screens Following Machine learning Mapping Navigational assistance Human learning Operations
Future	Biometrics Brain Computer Interface Multimodal input methods Localization Human-robot interaction

2.2 Robotic Wheelchair Hardware

2.2.1 Sensors

Robotic assistive devices are new concepts in urban environments. They play a vital role in assisting the community of people to reduce their physical load and allow for a stress-free lifestyle. Robotic wheelchairs assist the disabled in coping with with mobility in urban life. In urban environments, there are so many hazards that appear for wheelchairs where human assistance is very important. Biologically, the human body consist of organic sensors like the ears, nose, skin, eyes, and more. In the same way, a robotic wheelchair also needs such kind of sensors to sense the terrain for smooth navigation. For avoiding obstacles, robotic wheelchairs use sensors to perceive the environment's surroundings. A common type of sensor is the acoustic range finder. Sonar sensors can accurately measure objects at right angles or head-on. However, when the angle of incidence increases, less of the sound waves tend to

reflect toward the sensors. The noticeable effect is measured when the object is not large enough or smooth. Moreover, sonar creates cross talk effects which can produce more noise to adjacent sonar devices. Another frequently used sensor is the infrared (IR) range finder. IR sensors emit light, rather than sound, and sometimes gives false results with dark or light absorbent materials. This is similar to sonar devices having issues with sound absorbent materials. IR sensors also have difficulty with transparent or refractive surfaces. Despite their limitations, however, sonar and IR sensors are often used because they are small, inexpensive, and well understood. For robotic wheelchairs sonar or IR sensors are mostly well suited for identifying drop-offs, such as stairs and curbs. They are also not affected much by lighting conditions on the object surface. To get the reflected signal, it has to placed downwards to the terrain, but sometimes it can be hard to control the wheelchair within a few seconds to avoid an accident. Therefore, Laser Range Finders (LRFs) are more accurate for obstacle and drop-off detection. A typical LRF can provide a 270° view angle with a long range of about 1 meters. Two-dimensional scans within the plane of the obstacles in the environments can be detected. Examples of smart wheelchairs that use a LRF include the Rolland [29], MAid, and SCENARIO sensors. Unfortunately, LRFs are expensive, are large, and consume a lot of power, which makes the task of mounting enough of them on a smart wheelchair to provide complete coverage difficult. Another option is to use 3D LRF sensors to get a 360° view of the environment, but researchers are still finding alternative ways to use 2D sensors in robotic wheelchairs. Laser stripers can also be an option which, consists of a laser emitter and a charge-coupled device camera. They are inexpensive compared to LRFs, but can return false readings when the stripe falls on glass or a dark surface. Therefore, researchers often use in their wheelchairs (e.g., VAHM, TAO [14], OMNI, Rolland) a fusion of information from multiple sensors to locate obstacles. Researchers have always compensated the limitations of the existing sensors systems by using modified sensors or multiples sensors. But they are always trying to make them accurate, inexpensive, small, and invulnerable to environmental conditions. Moreover, researchers nowadays mostly depend on machine vision camera technology. Smart wheelchairs already use computer vision for landmark detection (e.g., Rolland, MAid, Computer-Controlled Power Wheelchair Navigation System [74]), and as a means of the head- and eye-tracking for wheelchair control (e.g., Watson, Mr HURI [42], Siamo). Undoubtedly. the cost of machine vision hardware has fallen significantly but time complexity is increased to detect the object categories. Robotic wheelchairs need faster detection systems to control their motors precisely and in a timely manner. Gyro sensors are

also another type of sensor used in robotic wheelchairs for identifying the surface plane information. They play an important role in wheelchairs when encountering uneven surfaces such as urban terrain. The following Table 2.2 shows a summary of the types of robotic wheelchair hardware currently used by the researchers.

Table 2.2: Hardware summary of the robotic wheelchair)

Hardware Types	Hardware
Short range sensors	Sonar IR sensors
Mid-term range sensors	2D LRF
Long range sensors	3D sensors LIDAR
Angular velocity sensors	Gyro sensors
Motor controller	PWM motor controllers Brushless motor controller Servo motor controller
Control devices	Joy stick Remote Voltage controller Speed controller
Machine vision	Wide-angle camera Fish-eye camera
Touch sensors	LED sensors Touchscreen

Figure 2.2: Conventional Laser Sensors

2.2.2 Conventional 2D Laser Range Sensor

The most commonly used 2D Laser Range Sensors (Fig. 2.2) are from HOKUYO and SICK. 2D LIDARs are popular sensing systems for challenging mapping, localization

(a) Sonar Sensor (b) 2D Laser Sensor (c) EMG Sensor (d) 3D Laser Sensor

Figure 2.3: Different types of sensors used in smart or robotic wheelchairs.

or obstacle negotiation tasks. The smallest and the lightest 2D sensor is manufactured by HOKUYO UST 10LX with maximum detection range up to 30m. It has a mid-detection range of 10m/20m, wide detection angle 270°, fast response 25msec, high angular resolution 0.25° (See. Fig. 2.4).

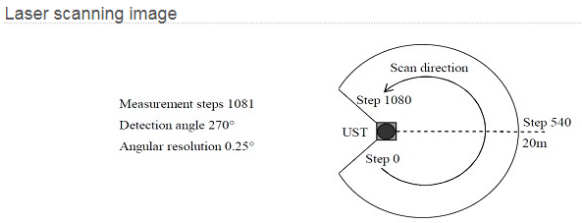

Figure 2.4: HOKUYO UST 10LX

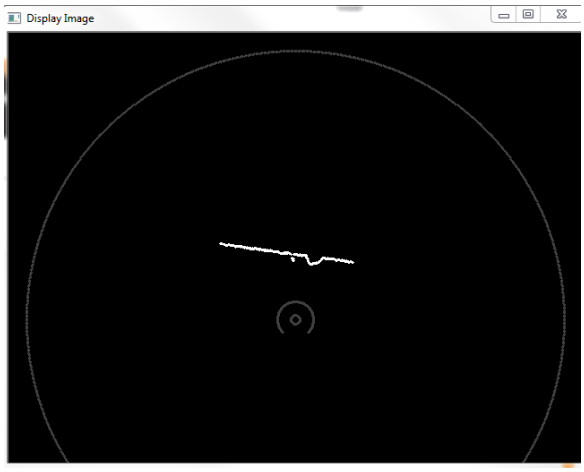

Figure 2.5: Sample output from 2D laser range sensor.

2.3 Mobility Functionality of Robotic Wheelchair

The mobility requirements of robotic wheelchairs depend on the type of task to complete. Some wheelchairs are for a specific task such as stair climbing, obstacle avoidance, and tracking companions. Some wheelchairs are autonomous and make instant decisions based on probabilistic measurements of features it gets from the environments like terrain condition recognition, vegetation detection on roadside, and so on. Although, robotic wheelchairs in this category are most appropriate for users who (1) cannot plan or execute a path to a destination and (2) spend most of their time within the same controlled environment. Other robotic wheelchairs such as the NavChair and TinMan had collision avoidance functionalities and spent most of the time in planning and navigation duties to the users. These systems do not use prior knowledge of the environments or any alternative specifications.However, user support is necessary for smooth navigation. Unfortunately, not all users can provide support for smooth navigation because they may have conditions such as major spinal cord injuries. In that case, a human companion guides the robotic wheelchair for navigation but this requires a lot of physical labour in uneven and unknown areas. Examples of wheelchairs that offer both autonomous and semiautonomous navigation are the VAHM, SENARIO, and SmartChair [47].

The multiple behaviors of the wheelchairs mobility depend on their specific set of tasks and input methods. For instance, three different operating modes are in the NavChair system, 1) indoor obstacle avoidance 2) doorways passing, and 3) corridor navigation. On the other hand, the Wheelesely, Mister Ed, OMNI, and Rolland systems offer support for task-specific behaviors. Though the NavChair uses a probabilistic reasoning model to combine information from the sonar sensors and a topological map to make adaptive decisions, it sometimes needs user manual control it due to uncertain terrain conditions. Moreover, task-specific robotic wheelchairs need autonomous control for performing actions. But in unknown environments, the wheelchair may have set to subtasks to accomplish a overall task such as in a hospital; multiple wheelchairs may track one nurse to follow for relocating their positions from one room another. For this instance, each wheelchair has to track the nurse's position as well as perform collision avoidance where multiple wheelchairs may have a different positions in the room. Therefore, navigation should be a combination of the activities of the wheelchair user's caregiving companion and robotic wheelchair itself.

2.4 Chapter Summary

This chapter presented different smart technologies for wheelchairs. It focused on two main properties: The human-machine interface and the navigation methods and devices. Also it reviewed other smart systems like monitoring and safety systems. From the review of many published papers, it is concluded that researchers are continuously trying to build powerful and helpful wheelchairs to ease the daily life activities and to give more independent mobility for people with different types of disabilities or aging problems.

Chapter 3

Terrain Recognition

Research interest in robotic wheelchairs is driven in part by their potential for improving the independence and quality-of-life of persons with disabilities and the elderly. However the large majority of research to date has focused on indoor operations. In this thesis, we aim to develop a smart wheelchair robot system that moves independently in outdoor terrain smoothly. To achieve this, we propose a robotic wheelchair system that is able to classify the type of outdoor terrain according to their roughness for the comfort of the user and also control the wheelchair movements to avoid sudden drop-offs and watery areas on the road. An artificial neural network based classifier is constructed to classify the patterns and features extracted from the Laser Range Sensor (LRS) intensity and distance data. The overall classification accuracy is 97.24 % using extracted features from the intensity and distance data. These classification results can in turn be used to control the motor of the smart wheelchair.

3.1 Introduction

In recent years, millions of people around the world have exhibited mobility impairments due to aging problems. Several robotic wheelchairs possessing user-friendly interfaces and/or autonomous functions for reaching given destinations have been proposed to meet the needs of an aging society [28],[40],[56],[22]. There are two kinds of wheelchairs that are used for the elderly or disabled people. Manual wheelchairs are widely used around the world by those who are able to control the wheelchair by hand. But it needs extra labor to control the direction of the wheel. Powered wheelchairs are more convenient to run but need a high level of attention to control the motor using a joy stick or remote control. Furthermore, such conventional control interfaces are sometimes forbidden by doctors for the elderly because of safety concerns. Thus the development of powered wheelchairs that can overcome doctors' safety concerns

would be of great benefit to many. In fact, [56] found that around 3 million people could benefit from such wheelchairs. Moreover, elderly wheelchair users are often accompanied by caregivers or companions. Thus, in designing wheelchair technology it is important to consider how we can reduce the caregiver's workload and support communication between user and caregiver [65]. Smart wheelchairs are a potential solution to these issues, which could also have the option of granting many elderly wheelchair users the independence of controlling their wheelchairs on their own.

Smart wheelchairs can be either driven by the user or computer system that can follow the caregivers movements to drive itself [33], [71]. Such a wheelchair follows the caregiver autonomously, by detecting the registered person in the system. But it is more important to detect the surface conditions as well for comfortable navigation in outdoor environments. We have found that the wheelchairs' terrain surfaces may be classified into four different categories. These are rough surfaces, watery places on the road, indoor plain surfaces, and dirt tracks. These roads may have different conditions which can be dangerous for the wheelchair user due to the risk of sudden accidents when driving over them. Suppose a wheelchair follows the caregiver but s/he misses hazards such as bumpy/pit areas. If the wheelchair were to not actively look for such hazards, it could fall and lead to injury of the occupant. Moreover, the motor speed of the wheelchair for different surface areas should not be same. It must be carefully handled by the wheelchair itself. For this reason, detecting the type of surface is a necessity. Another noticeable thing is that, for smooth movement, a wheelchair needs some surface information like the degree of roughness, which helps the system to control the speed of the motor. Although several improvements have been achieved in navigation for indoor settings, only a few proposed solutions are able to achieve safety and smooth motor control by looking at the surface road conditions in outdoor environments. The paper [15] obtained surface information about irregularities using a 2D laser for decreasing the burden to human workers on the road. Moreover, recent projects include an MIT intelligent wheelchair [52],[16],[1] which is able to navigate in indoor environments using voice-commands. The authors of [70],[41] developed a wheelchair which is able to assist the user for some household work. In [39], a map based localization approach was taken for outdoor navigation and the same work was extended to classify streets and sidewalks using grass information. Paper [26] studied accessibility in urban terrains and they found common environmental barriers for moving wheelchairs to mainly consist of steep ramps, rough terrains, and sidewalk irregularities. It is worth mentioning that all autonomous wheelchairs employ distance laser sensors and depth cameras but intensity data is also available

in the laser range sensor devices. This suggests that we can use all the available information provided by a laser sensor for effective indoor and outdoor navigational assistance to users. Specifically, our proposed system detects surface roughness using depth distance and intensity data. The intensity data is first used for classification of the path type such as flat, uneven, dirt tracks, and watery places on the road and then the wheelchair makes a decision to move-on, slow-down, stop, or avoid accordingly. In this part of our study, we used an ANFIS (Adaptive Neuro-Fuzzy Interference System) model for classification of surfaces and 3D elevation map (from distance data) generation for measuring the degree of roughness for our proposed wheelchair.

3.2 Surface Classification Methodology

The general block diagram of the whole procedure is shown in Fig. 3.1. We first, choose four types of common surfaces where the wheelchair is expected to navigate. For surface roughness detection, we give extra attention to distinguish between indoor and outdoor environments. In particular, we use the mean value of indoor roughness as a threshold to separate indoor and outdoor surfaces. We further categorize outdoor environments into three types, 1) dirt tracks, 2) asphalt roads, and 3) watery places on the road, which are shown in Fig. 1. For data observation, the wheelchair uses one ULM-30LX LRS in an orientation such that it can directly measure the distance to the surface as well as get the intensity value of any particular point in view. In our proposed system, the surface roughness is calculated using intensity data and corresponding angle of observation. The arrangement of the data collection tools in the wheelchair is illustrated in Fig. 3.3, Fig. 3.4, and Fig. 3.2.

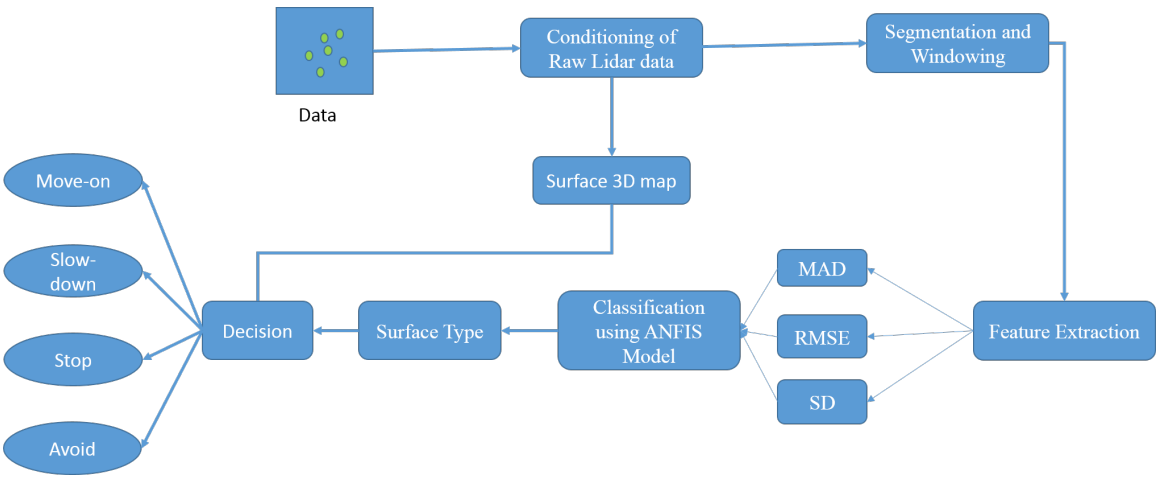

Figure 3.1: General block diagram of the whole procedure.

The pathways selected in our dataset consist of plain surfaces, uneven asphalt walk-way road surfaces, muddy areas, and also observed water on the road. The data was taken from the front region of the wheelchair as shown in the shaded triangle in Fig. 3.4. The great considerable thing is that the midpoint of the laser range sensor device always has a reflection point on the road's surfaces. So we consider the data around the midpoint segment for surface classification. The following subsections detail our surface detection approach.

3.2.1 Conditioning of Raw LRS data

All acquired data including distance and intensity pair $(inten)_i, dist_i$ were passed through the chi-square (χ^2) test using Eq. 3.1. This test is essentially used to filter outlier data from the sensor so that we can more accurately classify the type of the surface. We first collect some prototypical data of flat indoor surfaces, uneven surfaces from the roads, watery areas and dirt tracks in a control environment to get the expected value for each type of surfaces. Thus we find the mean ($\mu_{kthsurface}$), where k denotes the surface type. μ_k is feature vector that can be used in Eq. 3.1 to filter outlier sensor data for each surface type that we wish to detect. In addition, in order to avoid any undesirable artifacts, we also filter out data that has very high intensity or very low intensity.

$$\chi^2 = \sum (Observed - data - Expected - value)^2 / Expected - value \tag{3.1}$$

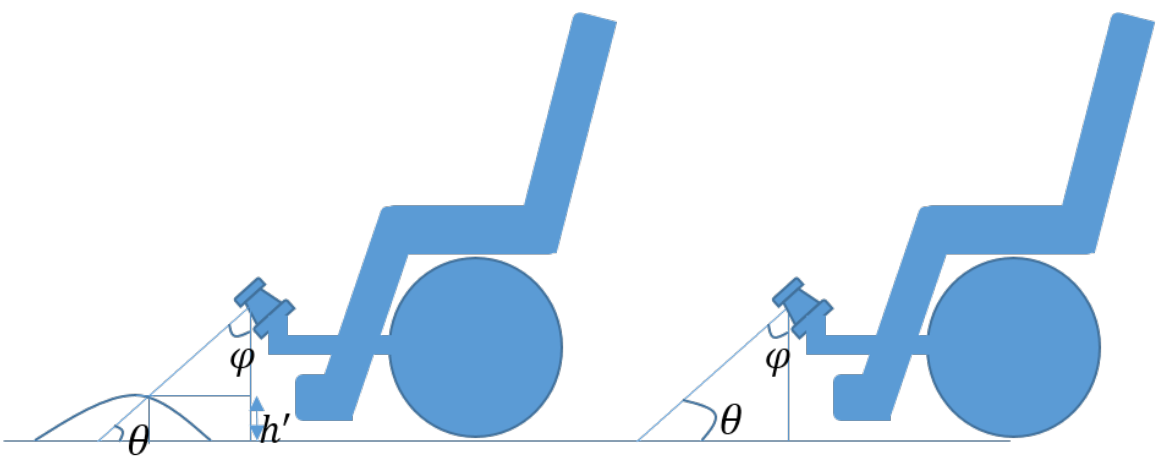

Figure 3.2: Arrangement of laser for surface roughness data calculation.

Figure 3.3: Proposed wheelchair system.

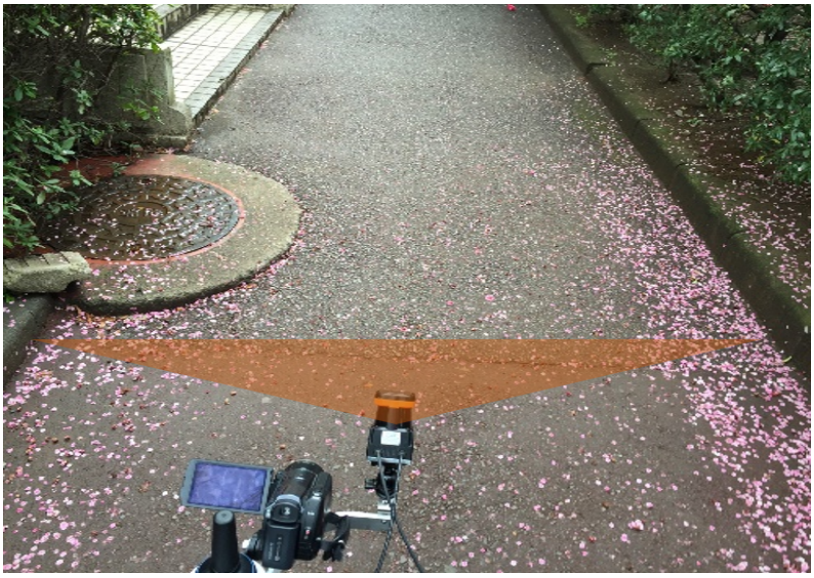

Figure 3.4: Data data collection apparatus.

3.2.2 Segmentation and Windowing

Using the entire LRS intensity data as input for pattern recognition and classification is not practical because the huge amount of data has high computational cost. To obtain the surface type the total scanned area is divided into small segments or patches. We define a surface patch S_k as a small region on the surface. Patch data block is 10×5 (data points by scanned time) which consists of intensity data and distance data points. The process of segmentation is repeated for checking whether the wheelchair is on a new surface or not. These patches are also used for generating a 3D surface map for measuring the roughness of the surface.

3.2.3 Surface 3D Map Generation

After preprocessing, we also create a patch-wise 3D elevation map of the current surface to measure the roughness of the surface and to find the possible running path of the wheelchair. For this, the surface roughness is calculated from the mean of the average height of the surface compared to the prototypical surface. The height of each pixel is not the same in uneven surfaces hence we calculate the height of the patch, plot a 3D map, and get the average roughness of the road according to Eq. 3.2. (Sample 3D maps from the first patch of different roads can be seen in Fig. 3.5.)

$$h^{'} = (dist_{i+1} - dist_i) \times \sin(\theta) \tag{3.2}$$

where, i is the scan sequence. Roughness is calculated by the Japanese industrial standard for R_Z, based on the five highest peaks and lowest valleys over the entire sampling length, which is formulated as Eq. 3.3

$$R_{ZJIS} = 1/5 \sum_{i=0}^{5} (h^{'}_{pi} - h^{'}_{vi}) \tag{3.3}$$

The surface roughness parameter results for different surfaces have been calculated using 3.3. The lowest roughness value can be seen in indoor places with a value of 27.8 and for road and dirt tracks and watery places we see 39.0, 85.5 and 43.2 respectively. Though this is not the most principled way to find the roughness of surfaces, we find it provides enough information for effective use of smart wheelchairs moving through rough terrain.

3.2.4 Feature Extraction

Feature extraction methods use segmented data as feature vectors. The feature must contain enough information of the data and must be simple enough for fast training and classification. The feature extraction method we chose is based on the best findings in [52] in which the authors showed that the most effective feature extraction for our task uses the Mean Absolute Deviation (MAD), Standard Deviation(SD), and Root Mean Square Error (RMSE) shown in Table 3.1. In addition, we use other features such as mean, standard deviation, the minimum value and maximum value of each surface for classification.

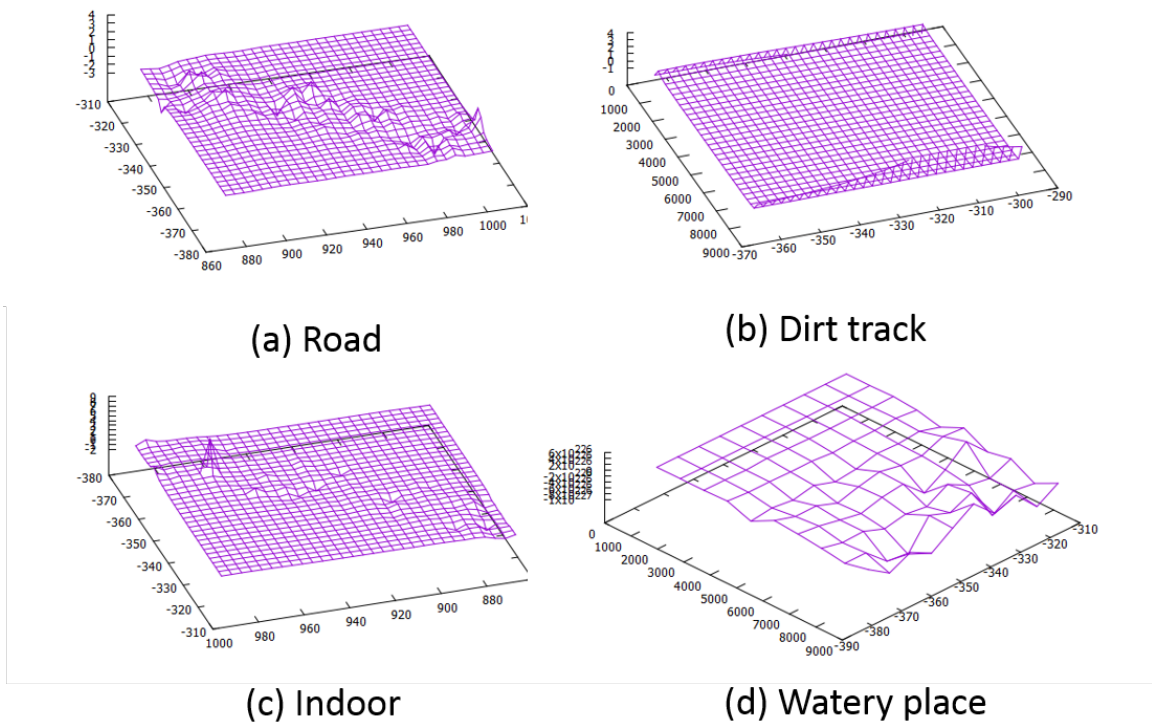

Figure 3.5: 3D elevation map from surface patches: (a) Asphalt road, (b) Dirt track, (c) Indoor, and (d) Watery places.

Table 3.1: Feature values of different types of surface data (intensity values)

	Watery	Road	Indoor	Dirt Track
SD	90.3	53	25.8	230.5
MAD	70.4	41.2	19.3	183.6
RMS	2525.5	3072.6	3447.3	4553.6

3.2.5 Classification Model

There are many techniques introduced and proposed in the field of machine learning for object classification such as the Multi-Layer Perceptron (MLP), Fuzzy C-mean (FCM), Adaptive Neuro-fuzzy Interference System (ANFIS), and Support Vector Machine (SVM). Any of these various learning methods could be used but we found ANFIS to be both fast and accurate. Real time decision making is especially vital for a smart wheelchair. For the ANFIS, Singular Value Decomposition is used to determine the number of fuzzy rules. The membership parameters of the Takagi-Sugeno-type ANFIS are adjusted by using a neural network. Fig. 3.6 shows the ANFIS structure with three input features, MAD, RMS, and SD denoted byI_i, where $i = [1, 2, 3]$ and there is one output, denoted by O_i [37]. Bell-shaped membership functions (MF) are used due to their advantage of being smooth, concise, and nonzero at all points. The required parameters for the input-output pairs are calculated using the hybrid backpropagation and least mean squares (LMS) algorithms. The membership functions are derived from four fuzzy rules and are given appropriate names (low, medium, and high). The output is calculated by using 3.4.

$$O = \sum_{i=1}^{L} [\frac{\prod_{j=1}^{p} MF_i^j(I_i)(Z_i)}{\sum_{i=1}^{L}(\prod_{j=1}^{p} MF_i^j(I_i))}] \tag{3.4}$$

where p is the number of linguistic variables and L is the number of rules in the rule base. The output of each rule, denoted by Z_i, is given by 3.5:

$$Z_i = \alpha_{i1} I_1 + \alpha_{i2} I_2 + ... + \alpha_{in} I_n \tag{3.5}$$

where $\alpha_i j$ is the consequent parameter of input$j$. The linguistic variable of the inputs is : MF_i^1: Low, MF_i^2: Medium and MF_i^3: High. The multiplexed output MF of the ANFIS is then fed to the speed controller program for controlling the wheelchairs motors.

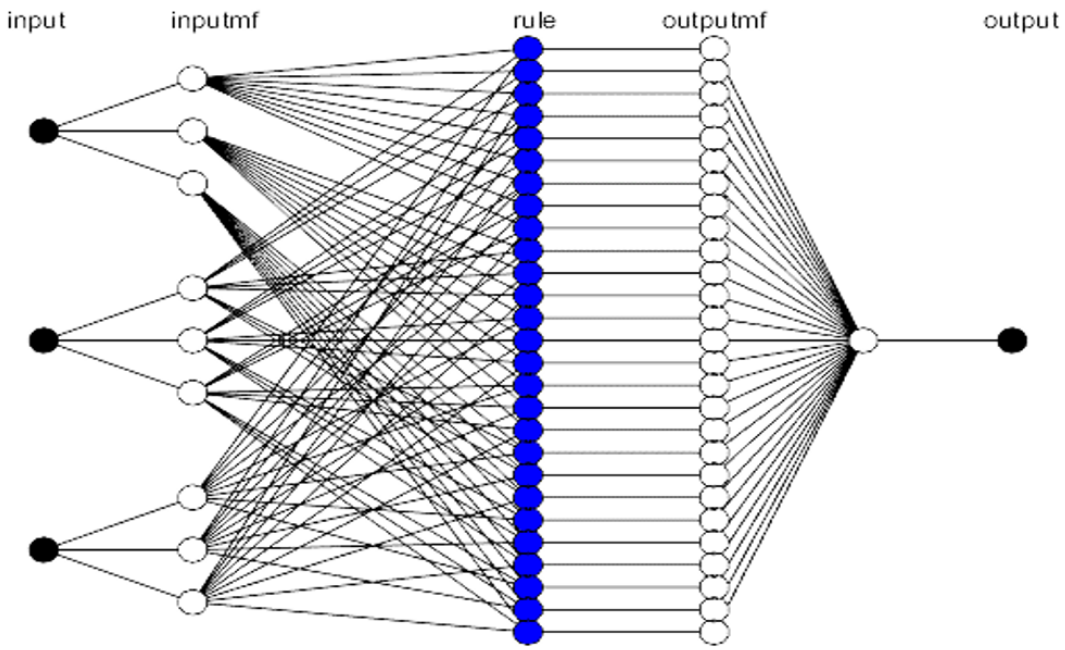

Figure 3.6: Structure of adaptive neuro-fuzzy inference system using neuro-Fuzzy Designer in Matlab with 3 inputs and one output.

3.3 Experiment and Results

In our experiment, we divided our terrain into four classes. All terrains were from the inside and outside of our research building. We chose an indoor corridor, outdoor asphalt walkway road connected to our building, muddy places from a playground and watery spots after rain, shown in Fig. 3.7.

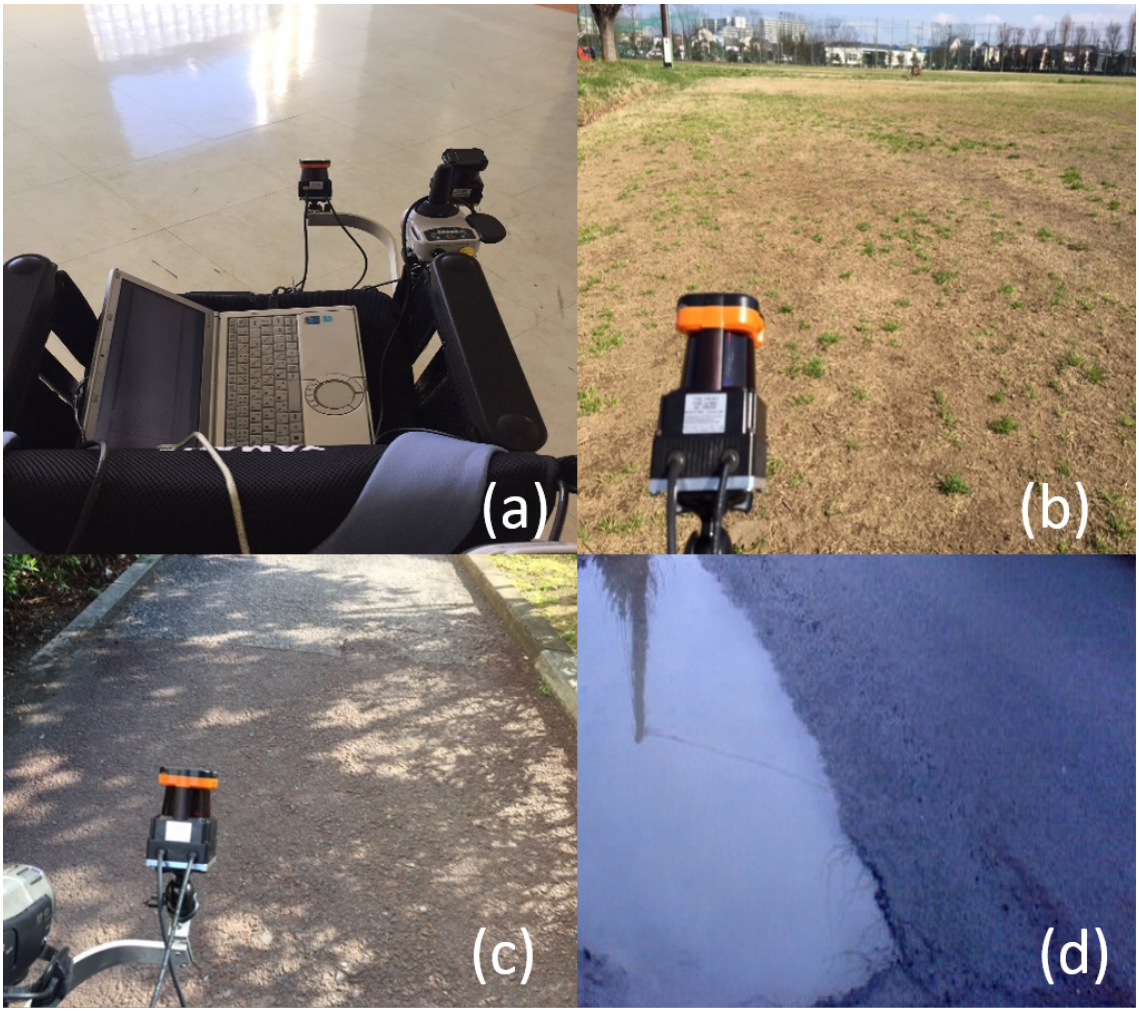

Figure 3.7: Example scene of data collection sites: (a) Indoor (b) Dirt track (c) walkway (d) watery places on the road after rain.

We segmented our data into two separate blocks and a total of 2000 data were taken at a time. For one block of data, 1600 were used for training the ANFIS classifier and 400 completely different terrain data were used for testing. As the LRS gave a large amount of intensity and distance data in a 200 ms time interval, we took only the middle portion data as described earlier in the segmentation and windowing section. Individual test procedures were performed to interpret the contribution of each LRS data. The tests were validated using several parameters which constituted the overall classification accuracy and were measured as the closeness between the actual class and predicted class using Eq. 3.6:

$$Accuracy = \frac{TP + TN}{TP + FP + FN + TN} \tag{3.6}$$

where TP and FP are the number of true and false classifications of a particular surface respectively. TN and FN are the number of true and false classifications of a surface identified by other surface and the correct surface, respectively. Table 3.2 shows the confusion matrix of our classifier on the different classes of surfaces. It is satisfactory that the identification of each surface is 96% on average except for watery places, which was perfectly classified. The misclassification rate is within the tolerance for the wheelchair to run through the surface. We note that [14] also achieved 97% accuracy in classifying the difference between streets and sidewalks however they did not consider the multiclass case. In our case, we achieve similar accuracies on multiple classes and even 100% on the watery case.

Table 3.2: Confusion matrix for the pattern classification method (4 classes for each test surface).

	Watery	Road	Indoor	Dirt Track
Watery	100%	0	0	0
Road	4%	96%	0	0
Indoor	3%	1%	96%	0
Dirt Track	1%	1%	1%	96%

The roughness of the surface is calculated using Eqs. 3.2 and 3.3. Using this roughness information the wheelchair can choose its terrain to move on. In our test cases, the surface class is identified correctly and the wheelchair is able to make appropriate decisions for navigation.

3.4 Chapter Summery

This chapter presented a method for terrain surface classification and roughness calculation using a single LRS sensor's intensity and distance data. The ANFIS classifier gave an overall accuracy of 97.24%. The combined results of classification and roughness are fed into the wheelchair motor controller for smooth running in urban settings. Moreover, the computed 3D surface elevation map could be used for making the decision of whether to move-on, slow down the speed or to avoid watery and muddy places on the road. We are also developing a wheelchair that can move on uneven surfaces by mechanically adjusted the positions of its wheel. We will implement the proposed method on this wheelchair so that it can autonomously detect surface conditions and move safely and smoothly.

Chapter 4

Single Laser Bidirectional Sensing

Research interest in robotic wheelchairs is driven in part by their potential for improving the independence and quality-of-life of persons with disabilities and the elderly. Moreover, smart wheelchair systems aim to reduce the workload of the caregiver. In this chapter, we propose a novel technique for 3D sensing of the terrain using a conventional Laser Range Finder (LRF). We mounted this sensing system onto our new six-wheeled robotic step-climbing wheelchair and propose a new step measurement technique using the histogram distribution of the laser data. We successfully measure the height of stair steps in a railway station. Our step measurement technique for the wheelchair also enables the wheelchair to autonomously board a bus. Our experiments show the effectiveness and its applicability to real world robotic wheelchair navigation.

4.1 Introduction and Motivation

In recent years, many people around the world have exhibited mobility impairments due to aging problems. According to the World Bank overview on disabilities [69], about 15% of the worlds populations experience significant disabilities. Currently the needs of many individuals with disabilities can be satisfied with powered wheelchairs. However, many disabled people have trouble when driving powered wheelchairs using standard joysticks or remotes. A clinical study [11] shows that 9% to 10% of people with severe disabilities have this issue. To recover their mobility, researchers have come up with robotic concepts for wheelchairs that can autonomously perform their functions. Indeed, several assistive wheelchairs possessing user-friendly interfaces and/or autonomous functions for meeting the needs of the disabled and an aging society have been proposed [28][40][56][65]. Robotic wheelchairs should be able to assist their users in avoiding obstacles for collision-free travel, going to pre-designated

places, and maneuvering through doorways or other narrow and crowded premises. In addition, such smart wheelchairs would be more helpful if they could follow their users caregiver autonomously; by detecting the registered person in the system hence reducing the workload of the caregiver [27]. However, most robotic wheelchairs are currently used in indoor environments to navigate through doorways or corridors while avoiding obstacles. Nevertheless, robotic wheelchairs should provide navigational assistance in urban areas like roads and rail or bus stations. Our previous work [36] was to detect any given terrains smoothness and recognize categories of the terrain like muddy, watery or rough places. The primary concern in developing outdoor navigating robotic wheelchairs is the safe navigation through a given path. Therefore, it is important to detect the types of terrain while traversing urban outdoor pathways. We found that our smart wheelchair successfully detected four classes of terrain with a success rate of 97% which helps maintain smooth outdoor navigation. However, there are many more important and difficult barriers along a given path that a given robotic wheelchair should have to detect for safe and smooth autonomous operation. In addition, smart wheelchairs intended to run autonomously in environments designed for humans must also be able to climb up steps in order to say, board a bus or train. In this paper, we develop a new mechanism for robotic wheelchairs in collaboration with Toyota Motor Corporation and the University of Tokyo that can detect steps and have the capability to move on stair steps. We note that most robotic wheelchairs use one or more 2D laser devices and vision systems to avoid hazards like narrow passes, slopes, and stairs. [34]. In particular, much of the previous work concerns the use of 2D Laser Range Finder (LRF) sensors for obstacle detection. However, using multiple sensors or any moving mechanism for sensing results in a more complex system thus increasing cost and the need for maintenance. But if one were to naively use a single laser, it would not provide enough information to properly sense the environment. In this paper, we propose a novel concept for sensing with a single 2D laser sensor that can obtain horizontal and vertical scan data simultaneously. We show that our setup is highly effective for finding steps on stairs or buses, which allows for smooth climbing with our newly designed type of robotic wheelchair. As a prerequisite, the wheelchair has to be able to acquire accurate measurements of the steps on buses and stairs on the ground floor of a building or railway station. Regarding this, researchers are working on building accurate models for overcoming these difficulties [18]. They rely on 3D laser range data for finding a given stairs planar surfaces from the observed point cloud to reconstruct models of staircases. 3D mapping [73][44] shows that 3D sensors can be used for terrain mapping and

obstacle detection for smooth navigation. Obwald et al. [45] presented an approach to autonomous stair climbing with humanoids given a known 3D model of the whole staircase using a 3D laser. For accurate and faster detection of obstacles on the path of the robot, researchers are using 3D sensing devices on the top of their systems. At the same time, some researchers are finding ways to get accurate measurements of environments with the help of 2D LRF to lower system cost. In [50][60] the authors presented some 3D sensing systems using 2D LRFs. In those systems, multiple LRF sensors installed in different directions were mounted on a rotatable unit to sense environmental hazards or for terrain classification. Fujita and Kondo [13] developed a sensing system using an arm-type sensor movable unit, which can sense in horizontal and vertical spaces to model stairs and gaps. The authors showed that their robot could measure the step size of stairs fairly well. However, they had a 5.8% error in calculating the step height and width. In [17], researchers fused depth images and laser readings for detecting and climbing stairs using a mobile robot. Vision based wheelchairs are also used mainly for navigation and positioning of the wheelchair in outdoor environments [61][2]. In this section, we propose a new robotic wheelchair in collaboration with Toyota Motor Corporation and the University of Tokyo [21], which can measure and climb stairs, escalators or board buses. Here, we also discuss a vision-assisted system to give navigational information to the user by mapping the laser data onto video images so that for example, people with partial visual impaired can benefit from seeing what the robotic wheelchair senses. The visual display of the laser data to the user can also be beneficial when driving the wheelchair in manual mode. We achieve all this with a novel approach where we use a single 2D sensor that is capable of sensing the outdoor environment, simultaneously in the horizontal and vertical directions.

4.2 Robotic Wheelchair System

Fig. 4.1 shows the mechanical design of the wheelchair, developed by Toyota Motor Corporation and the University of Tokyo. We incorporate our new outdoor environment sensing system on this new type of six-wheeled robotic wheelchair equipped with four hydraulic suspensions for lifting itself. Fig. 4.1 shows that the front wheel and middle wheel are attached to the suspension. When the wheelchair finds a step to move on, its control system lifts the front wheel onto it, while the rear and middle wheel balance it. Once the front wheel is able to maintain a good grip on the upper step, the middle wheel is lifted up and moved forward while balancing itself with the

help of the rear wheel. The schematic workflow in Fig. 4.2 describes the operation of these wheels. Moreover, the new robotic wheelchair is equipped with data sensing devices in addition to its control unit. The wheelchair comes equipped with a standard webcam (iBuffalo) with our novel 2D laser range setup using a HOKUYO UTM-30LX unit installed at 75cm above the ground plane. Detailed measurements of bus steps or stairs can then be obtained using the laser sensor so that information can be mapped onto a video display that is linked with the webcam, for the users benefit. With the measurement of the heights of steps on buses or stairs from the ground level, the wheelchair can then be autonomously commanded to climb the sensed height if necessary.

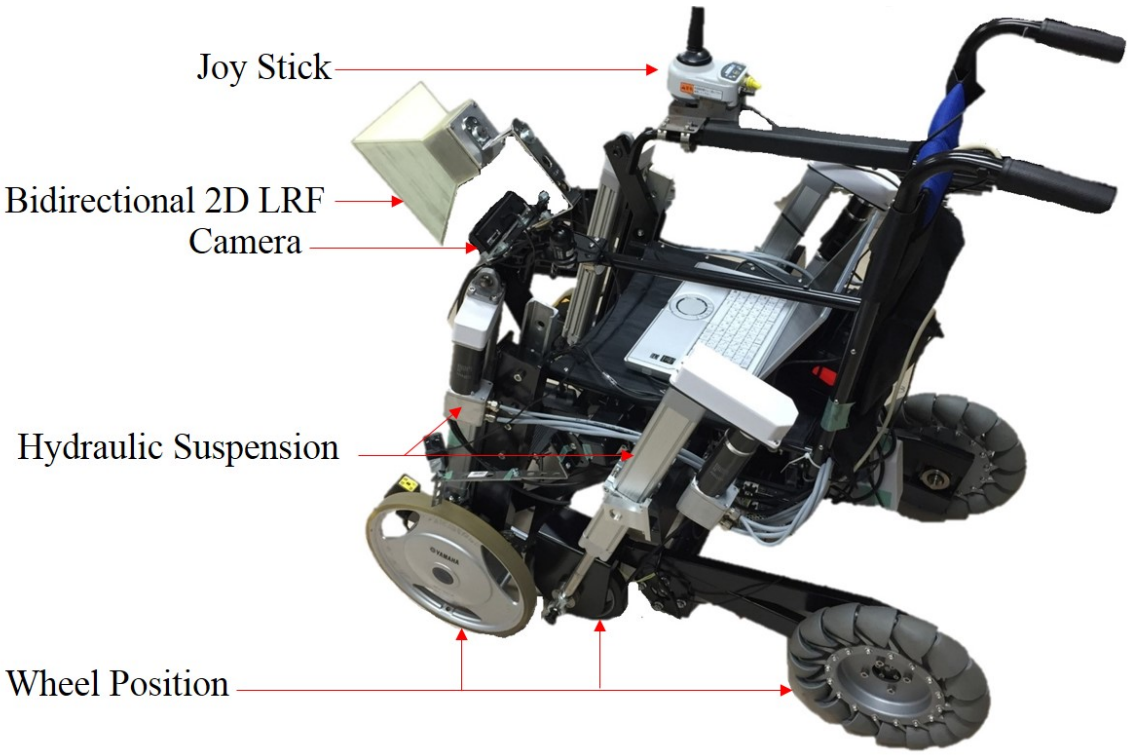

Figure 4.1: Robotic Wheelchair

4.3 Data Acquisition Method

For smooth navigational support of our new wheelchair, we propose a novel approach for data sensing using a single 2D laser sensor and undistorted mirrors. Mounting this setup, we can scan both the horizontal and vertical data along the wheelchair's path.

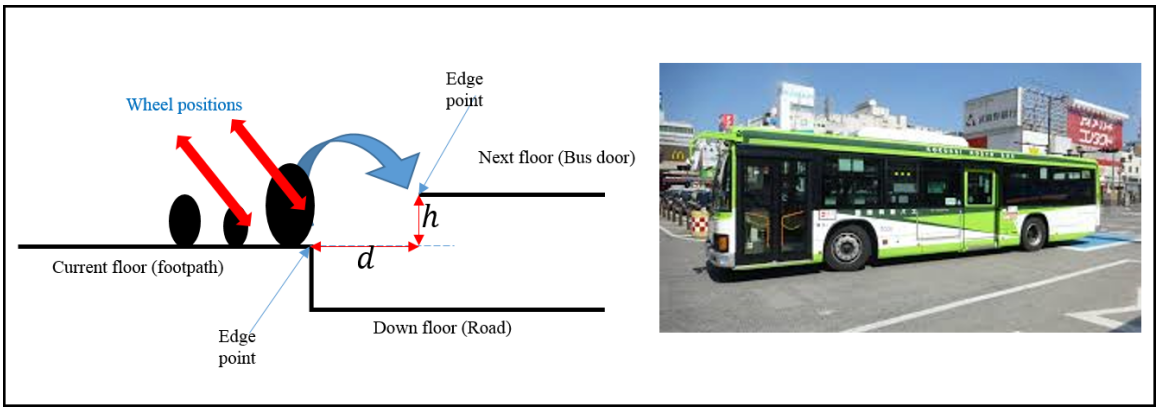

Figure 4.2: Schematic diagram of wheelchair wheel positions for boarding a bus.

4.3.1 2D Sensor Using Undistorted Mirrors

Conventionally 2D laser sensors have a wide angle horizontal field of view. We use a 2D LRF (HOKUYO) that has a horizontal angle view field of 270°, with a measuring interval angle of 0.25°. A single scan from the LRF captures 1080 values in 25 ms, representing a viewing angle of 270 degrees but we do not need to scan all 270° in the horizontal field of view. However, we do need some vertical scan data to detect steps. Thus, we divided the total view angle into three parts with a 90° view angle each by using three undistorted reflecting mirrors. Fig. 4.3 shows the data acquisition apparatus, equipped with a HOKUYO UTM-30LX and three undistorted reflecting mirrors. The mirrors are placed at 45° angles around the 2D laser device.

The collected data from the single LRF and three mirror setup is divided into three different segments where each mirrors associated data block consists of 360 values. The vertical scan data comes from the left and right side of the laser and the horizontal scan comes from the top of it. From the LRFs scan, the first block of 360 values corresponds with the left side mirror within the 0° to 90°, the middle block of 360 values are the angles between 90° to 180° , and the last block is from the right mirror corresponding to the 180° to 270° angles. The data that comes from boundaries between blocks are not reliable due to adjustments of the mirror. Therefore, we took values from the middle 20° of each block. Fig. 4.3 and Fig. 4.4 show the schematic view of mirror arrangement and corresponding scan lines of our novel technique for laser based data collection. In this orientation of the laser, the top data comes from $xy - plane$, where $(x, y) \in 360 < i < 720$; the right data and left data comes from $yz - plane$, where $(y, z) \in 0 < i < 360$ and $1080 > i > 720$ respectively.

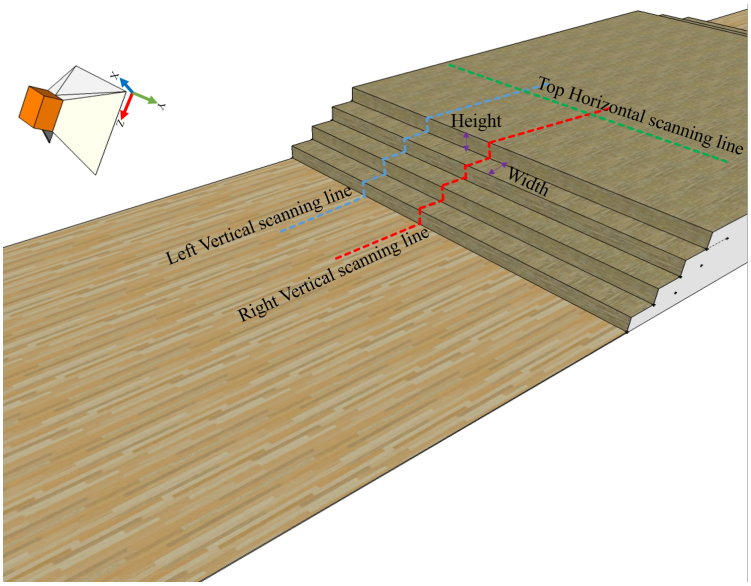

Figure 4.3: Schematic Diagram of Our Sensing System.

4.3.2 Coordinate Transformation from Laser Data to Camera Image Plane

Mapping the LRF data on the image plane would be important for displaying information on what the wheelchair senses to the users. For example, people with partial visual impairment could benefit from seeing the data on paths in front of them and could act accordingly while seated on the wheelchair. The staircases or buss door captured by the LRF has distance information, while the camera has the optical information projected onto the camera plane. Thus the LRF data needs to be appropriately mapped to the cameras coordinate system. In this paper, we divided conventional horizontal scanning LRF data into three different segments, each representing different 2D planes. Therefore, the coordinates of each block need to be transformed accordingly to the camera coordinates. We use the approach described in [62] for each block of our LRF data to map onto the image plane and for completeness, the approach summarized here.

Here, the LRF coordinates system of each block is denoted $f(x_t, y_t, z_t)$, the coordinates of the camera image plane is $c(u, v)$, and world coordinate system is $W(x_c, y_c, z_c)$. The most widely used camera model is the typical pinhole camera. The equation of the model is as shown in (4.1):

$$\begin{bmatrix} u \\ v \\ 1 \end{bmatrix} = \frac{f}{z_c} \begin{bmatrix} k_u & 0 & \frac{u_0}{f} \\ 0 & k_v & \frac{v_0}{f} \\ 0 & 0 & \frac{1}{f} \end{bmatrix} \begin{bmatrix} x_c \\ y_c \\ z_c \end{bmatrix} = \frac{1}{z_c} \begin{bmatrix} f_u & 0 & u_0 \\ 0 & f_v & v_0 \\ 0 & 0 & 1 \end{bmatrix} \begin{bmatrix} x_c \\ y_c \\ z_c \end{bmatrix} \tag{4.1}$$

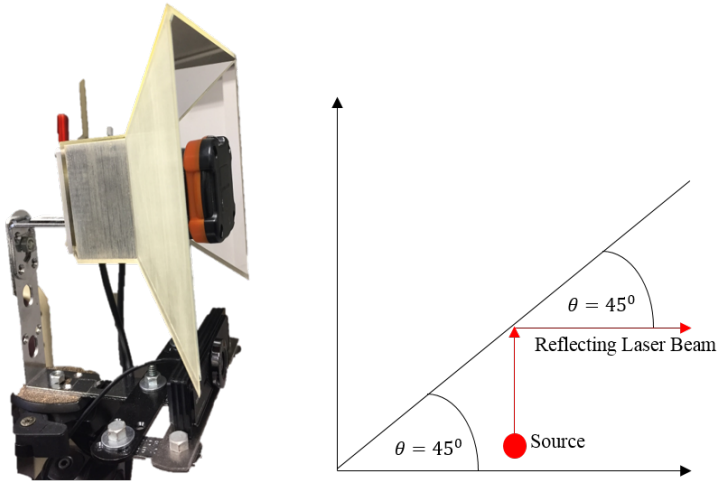

Figure 4.4: Sensing apparatus using HOKUYO UTM-30LX with reflecting mirror.

where u, v represents the coordinates of the image plane and x_c, y_c, z_c are the world are coordinates of the steps for stairs or buses. Here, the camera coordinate system is also considered. The scale factors k_u, k_v along the axes of the pixel coordinates are defined as the adjacent pixels physical distance ratios in the horizontal and vertical directions, respectively in the images. Moreover, the coordinates of the image centeru_0, v_0 are in pixels, with f denoting the focal length. The orthonormal rotation matrix $[O] = f(\phi_1, \phi_2, \phi_3)$ and translation vector $[T] = (t_1, t_2, t_3)$ are combined for transforming from the LRF distance data points to the camera coordinates, and we obtain conversion equation (4.2) according to coordinate transformation rules:

$$\begin{bmatrix} x_c \\ y_c \\ z_c \end{bmatrix} = \begin{bmatrix} \omega_{11} & \omega_{12} & \omega_{13} \\ \omega_{21} & \omega_{22} & \omega_{23} \\ \omega_{31} & \omega_{32} & \omega_{33} \end{bmatrix} \begin{bmatrix} x_t \\ y_t \\ z_t \end{bmatrix} + \begin{bmatrix} t_1 \\ t_2 \\ t_3 \end{bmatrix} \tag{4.2}$$

Therefore, substituting Eq. (4.2) into Eq. (4.1), the laser points coordinates are trans-formed into the camera image coordinates as,

$$\begin{bmatrix} z_c u \\ z_c v \\ z_c \end{bmatrix} = \begin{bmatrix} f_u & 0 & u_0 \\ 0 & f_v & v_0 \\ 0 & 0 & 1 \end{bmatrix} \cdot \begin{bmatrix} \omega_{11} & \omega_{12} & \omega_{13} \\ \omega_{21} & \omega_{22} & \omega_{23} \\ \omega_{31} & \omega_{32} & \omega_{33} \end{bmatrix} \begin{bmatrix} \cdot x_t \\ y_t \\ z_t \end{bmatrix} + \begin{bmatrix} f_u & 0 & u_0 \\ 0 & f_v & v_0 \\ 0 & 0 & 1 \end{bmatrix} \cdot \begin{bmatrix} t_1 \\ t_2 \\ t_3 \end{bmatrix} \tag{4.3}$$

According to Eq. (4.3), the world coordinates are $z_c = \omega_{31} x_t + \omega_{32} y_t + \omega_{33} z_t + t_3$, so the points of the LRF mapping onto the camera images is successfully completed.

4.3.3 Positioning the Laser Data onto the Camera Image Plane

Fig. 4.5 briefly explains the process of data plotting onto the camera image plane. For our new wheelchair system, we employed it for displaying the calibrated image for the wheelchair users comfort and assistance in manual navigation. The LRF data is expressed in the polar coordinates of two different planes, namely the $xy - plane$ for the top mirror distance values and the $yz - plane$ for the left and right mirror distance values. The laser distance data of the top mirror are then converted to 3D coordinates as,

$$x_i = d_{dist} cos\theta$$
$$y_i = d_{dist} sin\theta$$
$$z_i = 0$$

The data from the mirrors corresponding to the $yz - plane$ are converted in a similar manner. The extrinsic parameters are used in the experiments as follows:

$$\begin{bmatrix} x_{pos} \\ y_{pos} \\ z_{pos} \end{bmatrix} = \begin{bmatrix} 19.29 \\ 10.84 \\ 22.60 \end{bmatrix}$$

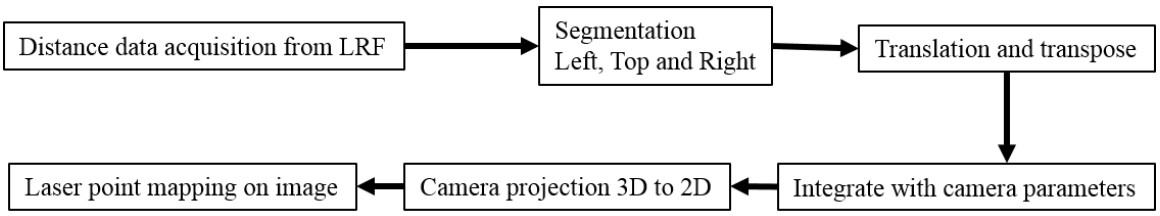

Figure 4.5: Schematic flowchart of laser data mapping on to the image.

In addition, the camera intrinsic parameters are defined as in Eq. 4.4,

$$k_c = \begin{bmatrix} fc_1 & \alpha fc_1 & cc_1 \\ 0 & fc_2 & cc_2 \\ 0 & 0 & 1 \end{bmatrix} \tag{4.4}$$

where the experimental values of camera matrix, $k_c = [0.213, -0.0455, 0.0019, -0.0002]$ and the focal length is , $f_c = [310.5370, 310.5219]$; the principal point is, $c_c[307.0099, 226.8956]$ and the skew coefficient, $\alpha_c = 0$.

As the LRF is placed in the middle of the mirror triangle, the single laser sensor acts as the equivalent of three lasers where the left and right side reflections from

Figure 4.6: Real time fusion results from video images.

the mirrors are denoted as vertical scanning and the top reflection is denoted as the horizontal scanning LRF. In addition, the top reflecting data comes from the $0.5z_i$ direction, and the left and right reflecting data are from $-0.5x_i$ and $0.5x_i$ directions in the world coordinate system respectively. The normal vector of the top part is in the positive z directions and left and right parts are in negative and positive x directions, respectively. After translation and transposing of our laser data according the camera parameters for the three segments, we plotted our data on to the image plane. The real time fusion results for the staircases are given in Fig. 4.6.

4.4 Step Measuring Methodology

Our proposed system will detect and measure the stairs or elevation gap for the bus door from roadside. Fig. 4.7 illustrates the overall methodology of measuring the step size of the stairs.

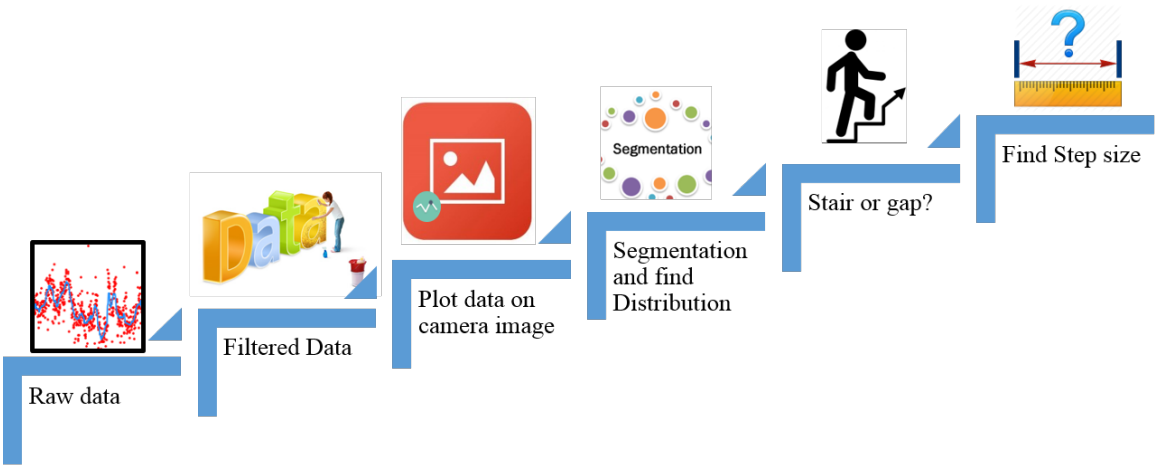

Figure 4.7: Methodology of finding the step size of bus and stairs.

All acquired data from the 2D laser had outliers removed so that we could accurately measure the step size of stairs or the elevation gaps of bus doors. In order to remove any undesirable artifacts, we use the median values and standard deviation of the data series. We also note, our bidirectional sensing device is titled towards the ground at 45° and 100 cm away from the stair or bus. We calculated the slope of the laser data to find whether it is positive or negative. A positive tangent indicates a planar surface and negative slope indicates steps. Moreover, for stairs the slope of the steps changes in intervals. As mentioned earlier, our sensing laser gives two vertical scan lines for the stairs. The left and right side data values are almost the same, as expected. For the vertical positional data, we get two distributions for every step of a given stairway in the $y - direction$ and the $z - direction$. Here, y and z indicate the horizontal and vertical spaces of the data plot respectively. $z - values$ give the height of the stairs where as $y - values$ give the width of the stairs respectively. The standard deviation and mean of each direction were used for finding the outliers. Then mode of the distribution of the values was applied to find the peak points and lowest point. The distance of those two point was then used to determine the height of the steps. For finding the mode, we used 1 cm interval in each direction.

4.5 Experiment Result

Several experiments were employed to confirm the effectiveness of our new sensing system for staircases and buses. The results for these experiments show that the pro-posed system is useful for sensing and measuring the step size of staircases and bus floor heights and widths from the ground.

4.5.1 Upward Stair Measurement

Fig. 4.5 shows an overview of the experiments environment. In this experiment, we consider the wheelchair to be located at the bottom of the staircase if it is 100 cm away from the first step. Each stair step is 26 cm wide and 17 cm high. From a stationary position, the wheelchair scans the data from the lasers left and right vertical mirrors. The top sensing mirror gives the distance of the wheelchair from stairs.

Table 4.1: Measurement of the steps (in cm) and error percentage.

System Calculation	Actual Values	Percentage Error
17.20cm	17cm	-1.16
26.42cm	26cm	-1.62
17.30cm	17cm	-1.75
26.28cm	26cm	-1.06
17.38cm	17cm	-2.21
25.59cm	26cm	1.58
16.44cm	17cm	3.31
26.60cm	26cm	-2.32

Table 4.1 shows the result with compare to ground truth values and experimental values of the stair height and width. It is an accurate measurement of the stairs suitable for our wheelchair to determine how it should move the stairs. Fig. 4.8 shows the data plot of the left vertical data from our experiment. Our sensing laser gives two vertical scan lines for the stairs. The left and right side data values are almost same, as expected.

4.5.2 Bus Floor

In Fig. 4.8, the vertical red line shows the height of the bus floor and the blue line shows the bus ground and body data distributions. We calculated the histogram distribution and the difference between peaks of the broken line. Our system calculated the value of the bus floor height to be 29.34 cm while the ground truth height is 30 cm. With this measurement, the new wheelchair can then climb onto the bus using the new wheel positioning system.

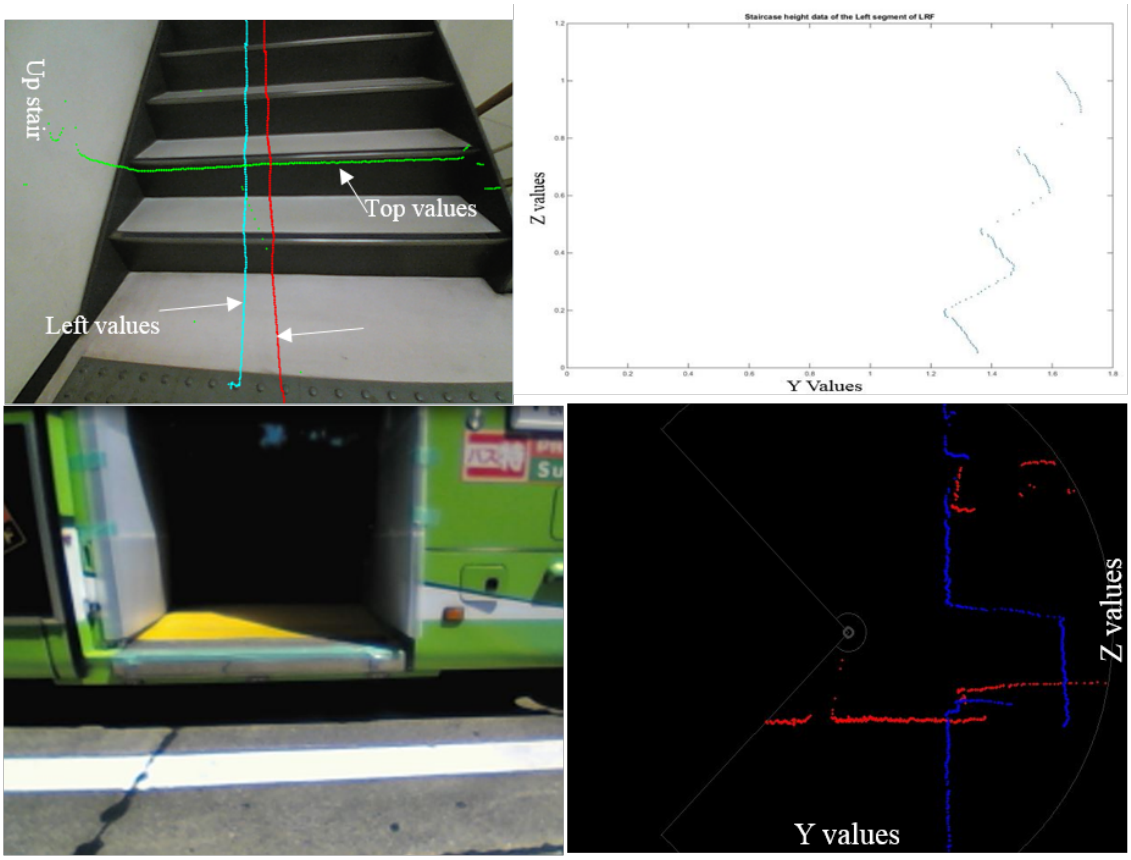

Figure 4.8: Methodology of finding the step size of the bus or stair.

4.6 Chapter Summery

This chapter proposed a novel 3D sensing system using a triangular shaped apparatus with undistorted reflecting mirrors for vertical and horizontal sensing of the floor. This sensing system is able to accurately measure bus or staircase steps for the purpose of climbing them. In contrast, such measurements are difficult with a single conventional 2D laser. Moreover, the experiment setup of this sensing system for our new six-wheeled wheelchair shows the effectiveness of the overall system for users to move about in outdoor terrains and onto steps such as those of stairways in railways stations or to board buses. Our next research goal is to make the wheelchair autonomously climb on steps by using the proposed sensing system.

Chapter 5

Bus Boarding Wheelchair and Autonomous Companion Following Mode

Research interest in robotic wheelchairs is driven in part by their potential for improving the independence and quality-of-life of persons with disabilities and the elderly. Moreover, smart wheelchair systems aim to reduce the workload of the caregiver. In this chapter, we propose a novel technique for 3D sensing using a conventional Laser Range Finder (LRF). We mounted two sensing systems onto our new six-wheeled robotic bus boarding wheelchair to locate the bus door and its determine its dimensions. Additionally, we have implemented a Single Shot Multibox Detector (SSD) to detect the bus stairsteps to allow for boarding. For precise movements, we successfully measure the height of the bus stairsteps and door width of the bus. Our step measurements and bus stairsteps detection technique for the wheelchair also enables the wheelchair to autonomously board a bus. Our experiments show the effectiveness and applicability of our system to real world robotic wheelchair freedom of movement.

5.1 Introduction

For bus boarding, wheelchairs need 3D measurements to get precise measurements of the doorstep's height and door width. Vision based systems can be a good option for this kind of information [57]. A 3D depth camera can also be used for terrain mapping with depth information. But for outdoor applications, saturation issues may occur due to sunlight. Moreover, the computational cost can be too high for real time applications in bus boarding robotic wheelchairs and the measurements may be inaccurate.

Figure 5.1: Bus boarding robotic wheelchair with new sensing mechanism.

Moreover, the wheelchair can acquire accurate measurements of the bus stairsteps and width of the bus door with updated laser sensing devices. Regarding this, researchers are working on building accurate models to overcome these difficulties with 3D laser sensors [18]. They rely on 3D laser range data for finding a given stair's planar surfaces from the observed point cloud to reconstruct models of staircases. Additionally, 3D mapping [44][34] can be a good tool for terrain mapping and obstacle detection for smooth navigation. But the price of such 3D sensors may prohibit deployment of current robots in real applications.

For precise movement of the smart wheelchair, it is very important to identify the observable area ahead of the wheelchair with faster detection tools. However, we note that most robotic wheelchairs use one or more 2D laser devices to avoid hazards like narrow passes, slopes, and stairs. [34] . In particular, much of the previous work concerns the use of 2D Laser Range Finder (LRF) sensors for obstacle detection. However, using multiple sensors or any moving mechanism for sensing results in a more complex system, thus increasing computational cost and the need for maintenance. Although, instead of using 3D sensors, in [59] the authors presented some 3D sensing systems using 2D LRFs. In those systems, multiple LRF sensors installed in different directions were mounted on a rotating unit to sense environmental hazards or for terrain classification. Fujita and Kondo [13] developed a sensing system using an arm-type sensor movable unit, which can sense in horizontal and vertical spaces to model stairs and gaps. The authors showed that their robot could measure the

step size of stairs fairly well. Likewise, they had a 5.8% error in calculating the step height and width, where our previous approach [35] of height measurement with a single bidirectional measurement sensor, yielded a 1% error, which is more acceptable for wheelchairs to board onto buses.

In this chapter, we propose a novel concept for sensing with a single 2D laser sensor that can obtain horizontal and vertical scan data simultaneously. To achieve bidirectional sensing, we have subdivided 2D sensors with 270° field of views into three equal segments. We attached three undistorted reflecting mirrors surrounding the sensor in each segment scanning path at an angle of 45°. In such an arrangement of mirrors, we virtually make the equivalent of three 2D sensors each with a 90° field of view. Moreover, we can install it in either way so that it can gives one vertical sensing lines and two horizontal sensing line or vice versa. In our previous works on step measurement techniques, we setup this system to get two vertical and one horizontal sensing lines as we used one system only to calculate precise step measurements of stairs.

For our Bus-boarding Mobility Robot (BMR) wheelchair, we used two Bidirectional Sensing Systems (BSS) to support the autonomous functionality of our robotic wheelchair, which can precisely measure the door's distance and height as well as board onto the bus. This system gives two vertical sensing lines by the wheels of our wheelchair to observe obstacles and from the horizontal lines, helps to find the height of the bus door. Moreover, the whole sensing system covers 1 m^2 of the area ahead of wheelchair to make observations for boarding. Through experiments, we found the vertical measurements along both sides of wheelchair provides an additional layer of safety to avoid collisions with the door while boarding. We also show that our setup is highly effective for finding steps on stairs, which allows for smooth climbing with our newly designed type of robotic wheelchair. Of course, a bus boarding wheelchair system needs to be able to detect the bus and bus door before boarding it. For that, we also installed a vision-assisted system to detect the bus and stairsteps of the bus with the help of a Single Shot Multibox Detector (SSD) [32] as its image recognition method.

5.2 System Overview

5.2.1 BMR Hardware

Fig. 5.3 shows the overall system hardware setup of our bus-boarding wheelchair, the BMR. We deploy our BSS on this six-wheeled smart wheelchair equipped with

heavy suspensions for lifting itself. The wheelchair can move all its wheels according to the terrain and the BMR controller has functionalities to move forward, backward, and auto-board up onto stairsteps. Moreover, the wheelchair is equipped with a standard wide camera (iBuffalo) and two Laser Range Sensors (LRS) installed using a HOKUYO UTM-10LX unit at 75 cm above the ground plane and titled downward. Besides, for visualization of laser data, we map sensor data on camera image and the calibrated wide camera is install in middle of the sensors axis so that we can map two BSS data on camera image which is explained in sention IV in brief. Additionally, an Image Recognition System (IRS) is also deployed with the wheelchair to detect the bus, bus door, and doorstep. An intra-network system is built for the BMR, where the sensors, BMR controller, and Step Detection module are connected with a RJ-45 connector to a hub. The camera image is sent to the IRS for bus and bus door detection and sensor data is used for precise calculation of the bus door height and width. Although, the movement of the wheelchair partially depends on the IRS, once a bus and its door are detected, the wheelchair runs its step detection and position correction systems and autonomously instructs the BMR controller for boarding. A detailed description of the sensor system for precise measurement is in Section IV.

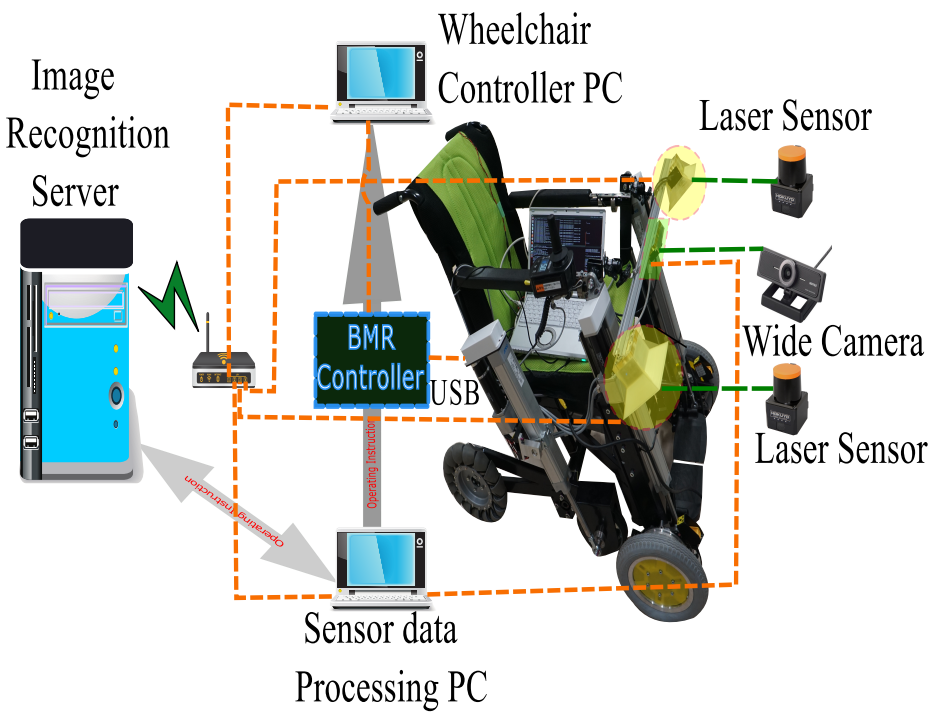

Figure 5.2: Hardware of Smart Wheelchair System

5.2.2 Detection Software

For devising a new bus boarding system, we need to be concerned with precise measurements of the door's location and height information. Before measurement, we have to locate the bus first for initial information gathering about the bus and bus door location. To do so, a camera vision system is used for detecting the bus and its sub-parts for proper information. We can recognize the bus, bus door, and doorstep successfully with our IRS module. Section 5.3 describes our overall implementation of the IRS in brief. Fig. 5.2 illustrates the overall system flow of our bus boarding wheelchair's tasks where detection is the initial step via the vision system. For bus boarding, it is very important to measure the doorstep precisely otherwise the wheelchair could cause an accident while boarding. Therefore, after doorstep detection, we use the sensing mechanism to get accurate measurements of the door width and the doorstep height from the ground is calculated. Completing these steps, the measurement module of our software sends instruction to the wheelchair to get its distance from the bus door and boards. The BMR has its own automatic functionality to operate its wheels to overcome the calculated height.

5.3 Bus, Bus door and doorsteps Detection

Nowadays, deep learning networks are better at image classification than humans, which shows just how powerful this technique is. As a prerequisite, the wheelchair has to be able to acquire detection of the bus at the bus stop and locate the doorstep for boarding. Regarding this, we note that semantic segmentation [67] of the image is very helpful for our purposes. In particular, semantic segmentation approaches[9] yield good solutions for object detection using a variation of Convolutional Neural Networks in which a new def-pooling layer and learning strategies such as in Region-based Convolutional Neural Networks or Deep Belief Networks are employed. Great strides have been made in recent years but processing speed still presents challenges to applications in realtime systems. That is why some researchers have proposed regression models [54] for deep learning to speed up processing time such as with YOLO and SSD. The authors of those papers proposed that they discretize the output space of the bounding boxes into a set of default boxes over different aspect ratios and scales per feature map location. At prediction time, the network generates scores for the presence of each object category in each default box and produces adjustments to the box to better match the object shape. Moreover, they frame object detection as a regression problem to spatially separated bounding boxes and associated class

probabilities. And they showed that their system runs at 59-67 FPS with mAP 76.85, which outperforms with other detection methods.

We used SSD for its high performance in precise bounding box location on the image and high 67 FPS speed. They use a multibox technique to locate the object in the image and draw the box near ground truth values. For real time applications, its not feasible to install it on the wheelchair so we use a pre-trained model for bus class identification and run it on a server. The wheelchair controller PC is connected to it remotely so that it can send a frame to the server and get the detected frame for further step calculation. In total, 400 images were used for training our bus, bus door, and bus doorstep detectors. For bus detection, we observed 100% accuracy in training, whereas we only attained 82% and 88% accuracy for our validation test set of different types of bus detections (Fig. 5.4).This was not problematic as we observed that buses would eventually be detected in some frames so that once the bus is detected, wheelchair stops sending frames to server and can perform its boarding. We ran a real scenario as video on our server and it successfully located our classes on video (Fig. 5.5). We could also detect the doorstep from our mock-up bus using the IRS.

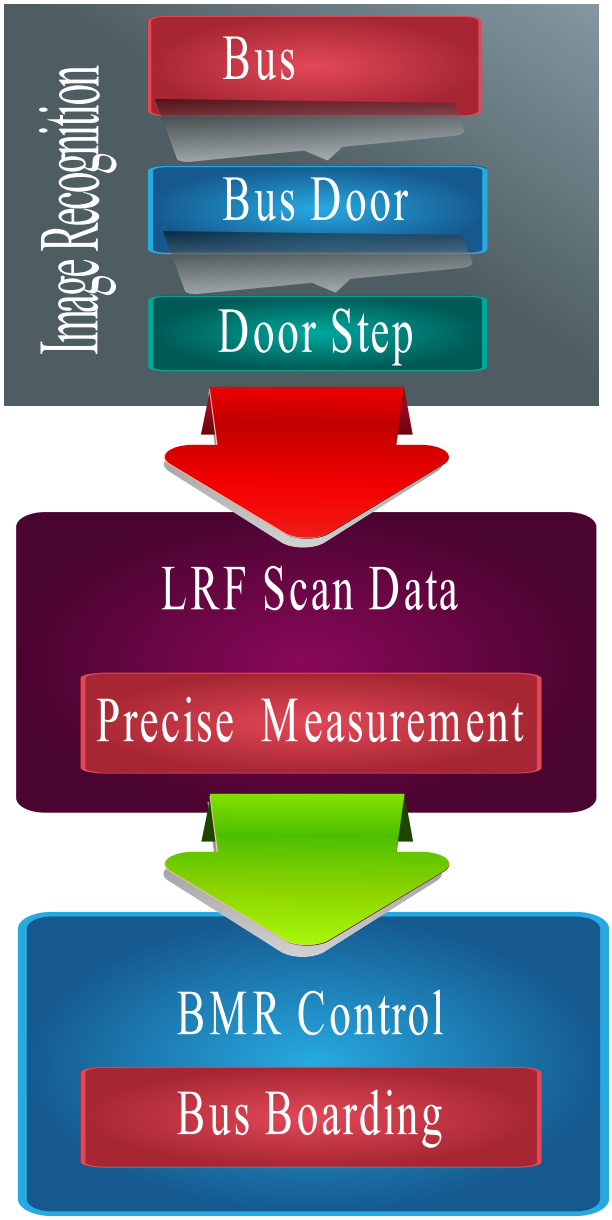

Figure 5.3: System Flowchart

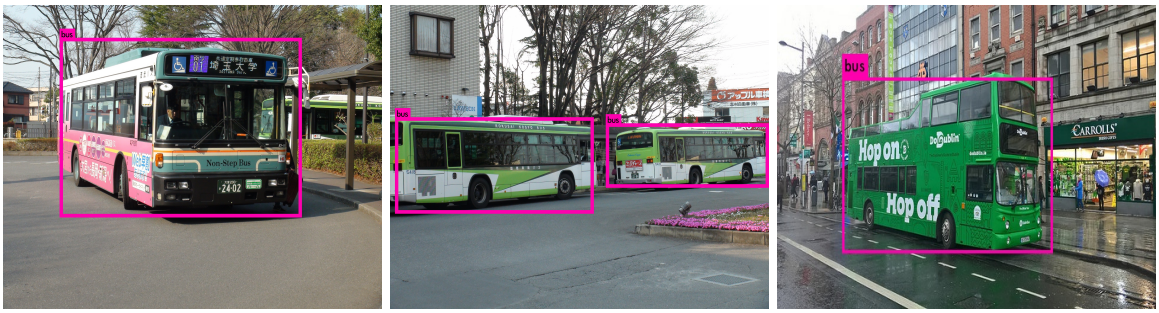

Figure 5.4: Different Types of Bus Detections Using SSD

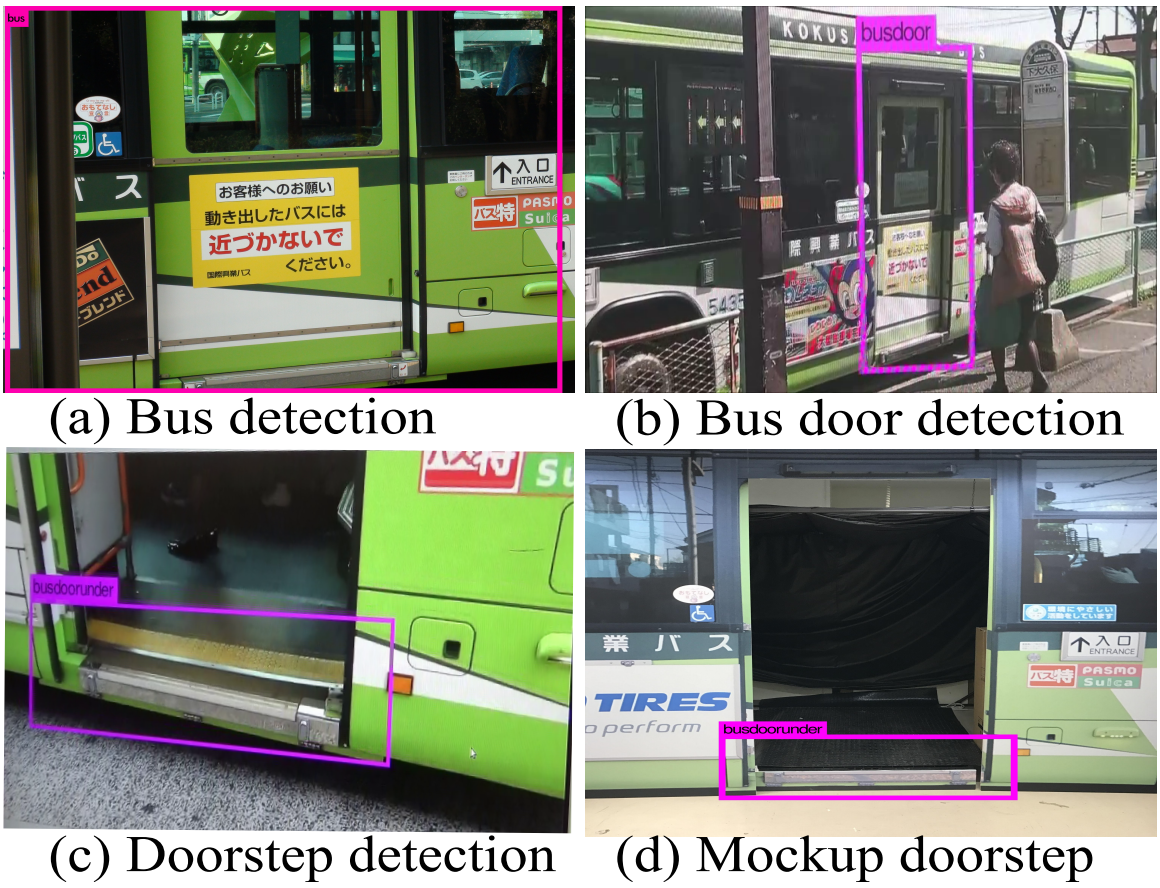

(a) Bus detection (b) Bus door detection

(c) Doorstep detection (d) Mockup doorstep

Figure 5.5: Image Detection Using SSD

We considered another issue is that, when a wheelchair is standing at a bus stop, it will observe a bus with a door status. It may be open or closed. Our system will also detect that status before activating its measuring system to get the height of the door. The wheelchair will only move when it gets the door is open. The result is shown in Fig. 5.6.

Figure 5.6: Open and Closed Door Detection

5.4 Bidirectional Sensing System (BSS)

5.4.1 Sensor System

In this section, we propose a new sensing mechanism using 2D laser sensors which can scan both in the horizontal and vertical directions. Conventionally, 2D laser sensor have a wide angle horizontal field of view. We use the HOKUYO 2D LRF with a horizontal field of view 270°, with a measuring interval angle of 0.25°. A single scan from the LRF captures 1,080 distance values in 25 ms but we do not need to scan all 270° in the horizontal field of view for measuring height. However, we do need some vertical scan data to detect steps. Fig. 5.7 shows the data acquisition apparatus, equipped with a HOKUYO UTM-10LX and three surrounding undistorted reflecting mirrors. The mirrors are placed at 45° angles around the 2D laser devices. The collected data from a single LRF is divided into three different segments where each mirror's associated data block consists of 360 values with angle coverage of 90°. From the LRF's scan, the first block of 360 values corresponds with the top side mirror

within 0° to 90°, the middle block of 360 values are the angles between 90° to 180°, and the last block is from the bottom mirror corresponding to the 180° to 270° angles. As a result, the single laser sensor functions as three virtual laser sensors, each with a 90° field of view. In the Fig. 5.7, the top and bottom part of the sensor shows two virtual horizontal scanners and one vertical. To avoid outliers, the data coming from the joint between two mirror segments is avoided. Therefore, we discard values from first and last 10° of each block. In this orientation of the laser, the top and bottom data from sensor in segment blocks 0 to 360 and 721 to 1080 are plotted in the $x - z$ plane and the vertical sensing data in the segment blocks 361 to 720 are plotted in the $y - z$ plane.

For bus boarding, we need two vertical scanning lines set apart at a distance the same as the wheelchair width so that it can avoid collisions with the bus door. Therefore, we use two BSS and equip them along the same axis on a 78 cm long bar edge tilted to the ground. This gives two vertical sensing lines from the far left and right of the sensors and four horizontal sensing lines across the vertical lines. Theoretically, we merge the horizontal data from the top and bottom so that we can receive a single distance value from both sensors. The vertical sensing positions of sensors start from 3 cm by the front wheels to check for obstacles.

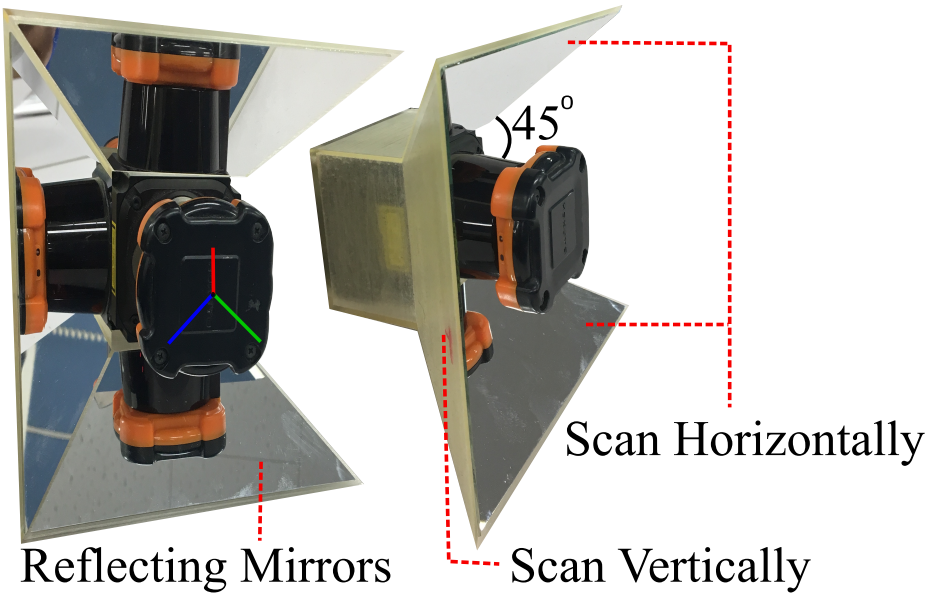

Figure 5.7: Bidirectional Sensing System (BSS)

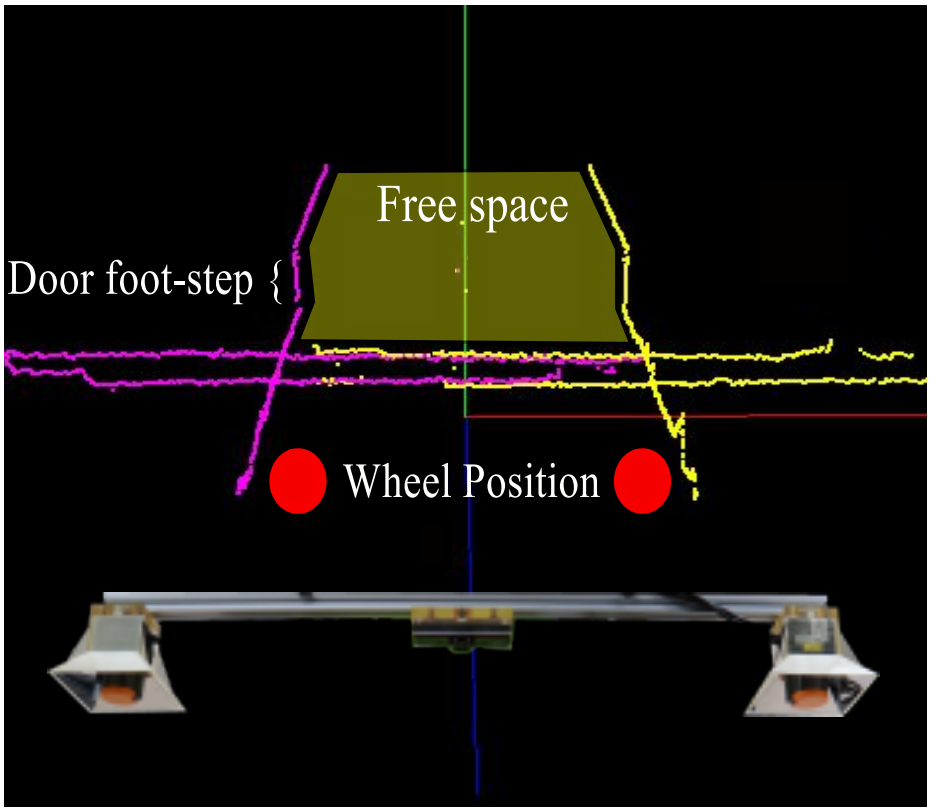

Figure 5.8: 3D Projection of Sensor Data

Our sensing area also covers 1 meter of distance ahead of wheelchair. The upper area of the top sensing line is important to find other obstacles like other passengers, bus seats, or luggage. When the wheelchair is instructed to board the bus, our system can sense this area as free to board, otherwise it sets itself back. This feature add an extra safety measure for our wheelchair. Fig. 5.9 shows a 3D projection of the scanning data when the wheelchair is docked in front of the bus door. The pink lines show what comes from the left sensor and yellow lines are from the right sensor. The free space for boarding inside the bus lies in between the two vertical lines above the top horizontal scanning lines.

5.4.2 Mapping Sensor Data on Camera Image

Mapping sensor data on the camera image plane is important for matching the bus doorstep detection on image for cross referencing with the scanning data values. Scanning data is used for step measurement and correcting the wheelchair position according to the door of the bus. In this setup, we divided our scanning data into three different segments to find the horizontal surfaces and vertical surfaces ahead of the wheelchair. The scanning data are stored in a point cloud as (x, y, z) values where x and y are calculated from distance values from the sensor using the following equation:

$$x = distanceData \cdot \cos\theta, y = distanceData \cdot \sin\theta \tag{5.1}$$

where θ is the angular value from which the distance data comes and $z = -75$, which is the actual height of the sensor position from the ground. Since the image is on a 2D plane, we need to project to 3D coordinates. Thus we translate our data according to the camera plane and store it in the point cloud. And finally, we plot this data according to the pixel position of the calibrated camera image. To achieve that, we calibrate our camera to find the relationship between world coordinates and 2D coordinate using the following equation:

$$\begin{pmatrix} u \\ v \end{pmatrix} = \frac{f}{z_c} \begin{bmatrix} k_u & 0 & \frac{u_0}{f} \\ 0 & k_v & \frac{v_0}{f} \\ 0 & 0 & \frac{1}{f} \end{bmatrix} \begin{bmatrix} x_c \\ y_c \\ z_c \end{bmatrix} = \frac{1}{z_c} \begin{bmatrix} f_u & 0 & u_0 \\ 0 & f_v & v_0 \\ 0 & 0 & 1 \end{bmatrix} \begin{bmatrix} x_c \\ y_c \\ z_c \end{bmatrix} \tag{5.2}$$

where, u, v represents the coordinates of the image plane and x_c, y_c, z_c are the world coordinates. The scale factors k_u, k_v along the axes of the pixel coordinates are defined as the adjacent pixels' physical distance ratios in the horizontal and vertical directions, respectively in the images. We also consider the camera's extrinsic parameter in our experiments to find the accurate pixel in the camera image is as follows

$$\begin{bmatrix} x_pos \\ y_pos \\ z_pos \end{bmatrix} = \begin{bmatrix} -0.0620 \\ -19.2916 \\ 75.4088 \end{bmatrix} \tag{5.3}$$

5.5 Experimental Setup

Our main goal of the experiment is to make our wheelchair autonomous and able to identify the bus and bus door while also being able to measure the bus door height precisely. For frequent experiments, it not always possible to test our system on a real bus. In our experiments, we set up a mock-up bus with printed image on a large sheet to simulate a real bus environment. Fig. 5.9 shows the setup of our mock-up bus for our bus boarding case study.

Figure 5.9: Mock-up Bus for Indoor Experiments

5.5.1 Step Detection and Position Correction

For bus boarding, it is essential to get precise measurements of the doorstep's height and door width. The doorstep's height is used for wheel movement in the upward direction and door width is necessary for avoiding collisions with the door's sides. Ideally, the bus's doorstep height and width would be approximately 15.0 cm and 110.0 cm respectively. For calculating the measurements, we took the horizontal scanning data from both sensor's top and bottom portions of the data. The top and bottom scanning lines are used for checking the height of the doorstep and door width. If both horizontal lines are in the same plane, then it is assumed that the wheelchair is running on a plane surface. Alternatively, if we observe over some threshold height i.e 12 cm, then the door is found. Moreover, if the wheelchair is docked straight to the door then the average distance from both sensor's end segments of the data is approximately equal, otherwise the wheelchair is on the left side or right side of the door. The determination of this fact depends on which sensor's distance data is less than the other.

Additionally, for measuring the door width, we applied a simple method where a dot product is used for calculating the width of the door. The horizontal data comes from top and bottom segment of the sensors and the total amount of data is 360 in each segment. We convert all the 2D data into 3D point cloud and take a patch of 5 data points. Then calculate the vector magnitude and dot product from 2nd point to 1st and 5th, which we called as feature for surface or door. If door appears on data it will gives 0 otherwise 1 or -1 as ideally, the angle between two vector in any patch would be $0°$ or $90°$ or $180°$. From first sensor we take first feature of door as a start point of door and second sensor gives us end point of the door. Then compute the Euclidean distance between these two points to get the actual width of the door.

5.5.2 BMR Control

We have been collaborating with Toyota Motor Corporation to make a smart wheelchair that can board buses and escalators to grant freedom of movement to users. The BMR is equipped with six motor wheels. For normal movements, the wheelchair uses the front and rear wheels while the middle wheels support its balance while boarding. The dimensions of the smart wheelchair are $72.0 \times 95.0 \times 72.0$ in cm. It can carry a typical weight of approximately 95 kg. The BMR can be controlled either via remote control or joystick. Although it can be manually maneuvered, we implemented autonomous control through programmed instructions with door detection from scan

data and control its movements. It has also the capability to automatically board buses based on any found height. We implemented our algorithm on it to find the bus and bus door with proper measurement of height and the door with the help of bidirectional sensing using 2D lasers.

5.6 Experiment Results

We conducted our experiments for bus boarding with a newly trained image recognition server that can detect buses and bus doors as well as doorsteps. Fig. 5.10 illustrates the outcomes of our system on camera images where we plot our sensor's data onto the image plane. The blue lines come from the left sensor and the cyan lines data come form the right sensor. The illustration shows the laser data in the 3D world space on the 2D images while the BMR approaches to the door. When the wheelchair observes a certain height (i.e. > 12 cm) wheelchair plays a sound indicating, "The door has been detected."The sound playing is another feature for our wheelchair to make other passengers aware and cooperate with the wheelchair for safe boarding. In Fig. 5.10(b), we see that the horizontal line aligns with the height of the door. After that, the wheelchair moves forward a little bit to correct its position for boarding where the horizontal lines are aligned flat as shown in Fig. 5.10(d). Fig. 5.11, depicts the actual moving of our wheelchair in six phases with boarding preparation. For boarding, the wheelchair lifts its front wheel to the height found using the laser sensor. The wheelchair then executes a series of movements to overcome that height and successfully board the bus. We have done this experiment by setting different heights of the doorstep and our wheelchair successfully detects the height and boards the bus.

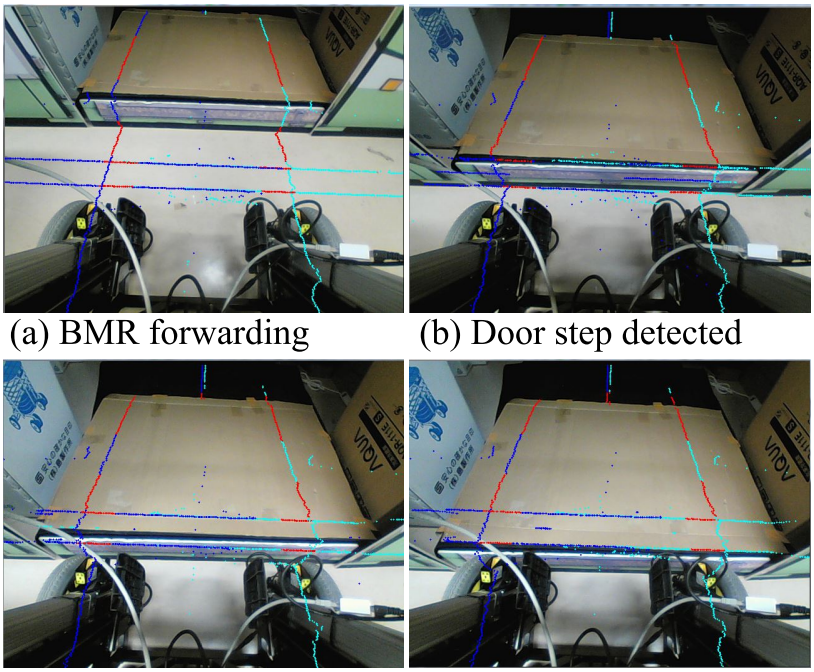

(a) BMR forwarding (b) Door step detected

(c) Adjusting for boarding (d) Boarding Instruction

Figure 5.10: Visual camera images for boarding: (a) Running State (b) Detected bus doorstep (c) Adjusting its distance for safe boarding (d) Boarding

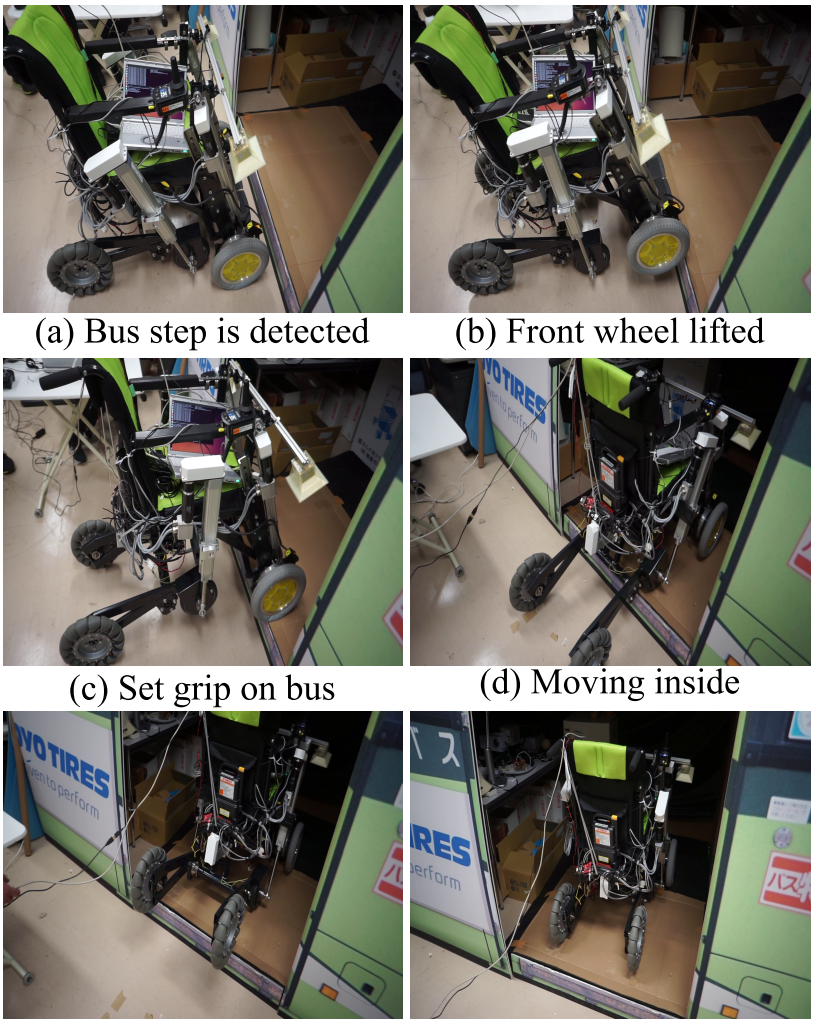

(a) Bus step is detected (b) Front wheel lifted

(c) Set grip on bus (d) Moving inside

(e) Lifting rear wheel (f) Boarding is completed

Figure 5.11: Our Wheelchair System Autonomously Boarding the Bus

Moreover, we also do experiments on real bus for boarding and disembarking. Where we set the real bus door height from the wheelchair ground is 15 cm. And our wheelchair successful measure that height for boarding (fig 5.12) and disembarking (fig 5.13).

5.7 Moving Alongside Companion

Our previous work in [27], used a particle filter framework to track the companion's position and orientation in terms of both the body and head to control our BMR position and speed with the companion. In order to move along with a companion, the ability to measure the companion's behavior is paramount. Whenever the companion moves only straight ahead or backwards, the wheelchair can follow the companion

Figure 5.12: Real bus boarding experiment

in a side by side formation by only considering his/her positional information. The companion is modeled with laser sensor data that is reflected from the upper part of the body. The laser sensor is placed horizontally at the companion's shoulder level. The contours in the data are shaped like parts of an ellipse. We interpolate this ellipse with center coordinates (u, v) and rotation angle ϕ. The tracking parameters are estimated in each frame by the particle filter that employs a random walk model for state propagation. The likelihood evaluation of the observation model is a score based evaluation with the following equation:

$$w_t{}^i = \exp -d_{max}{}^2/\sigma_d \tag{5.4}$$

where, $w_t{}^i$ is the likelihood score based on the laser image, and d_{max} is the maximum distance between the evaluation points and the nearest distance data. In every time instance, a distance image is generated from laser image to obtain each distance d_n. The variance, σ_d is calculated from d_n. The repeated likelihood evaluation procedure is obtained from each sample as shown in Fig 5.14. At each time t, the estimation of the state is derived as the expectation of the weights over the sample. Moreover, the companion sets his/her position on a laser image for initialization of wheelchair's tracking target. Autonomous registration of the companion is somewhat difficult using a laser sensor data. To simplify matters, we deploy a touch panel on the wheelchair where the companion registers him/herself for tracking. Additionally, losing track of the target does occur when the wheelchair moves in crowds or when

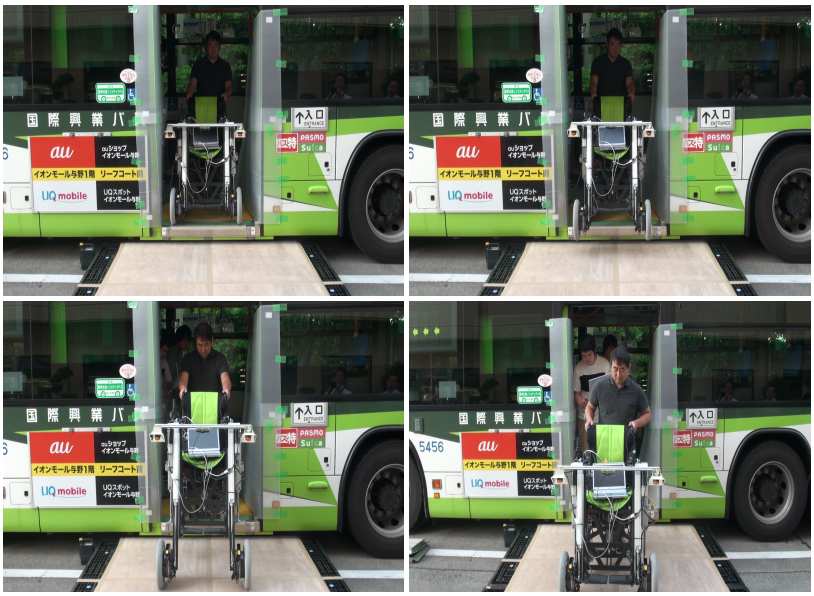

Figure 5.13: Real bus disembarking experiment

the companion bends his/her upper body to pick something. Therefore, we also use the color information of the companion and find the elliptical contour of nearest to the sensor for re-identification.

Moreover, for the following path calculation, we take the $X-axis$ as the left-right directional coordinates and $Y-axis$ as the forward-back operations of the wheelchair. Fig. 5.15 illustrates, the trajectories of the companion and the wheelchair, in which they move side by side. The speed is controlled by looking at the initial position of the companion and wheelchair. If the displacement $(\delta u, \delta v)$ is increased, then the speed is also increased and if the displacement is small, then the speed of the wheelchair motor is also slow to follow.

Our robotic wheelchair will track the companion/caregiver using this observation model and in each time instance, we calculate the likelihood evaluation by using the laser images from the sensor data. This companion following mode is continued until the wheelchair and companion reaches the bus station. While the wheelchair along with companion waits for the bus, the wheelchair changes its mode to AM mode to detect the bus and bus door.

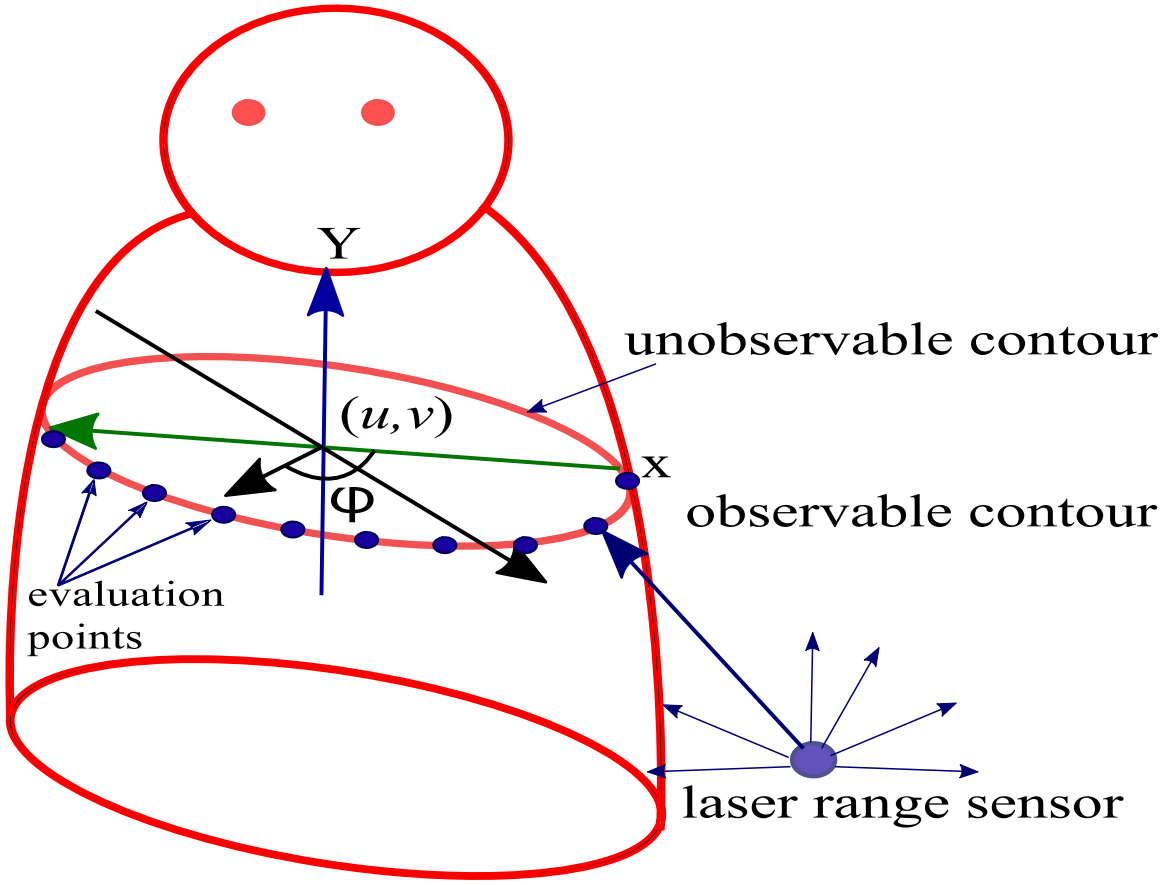

Figure 5.14: Contour observation model and likelihood evaluation by the laser.

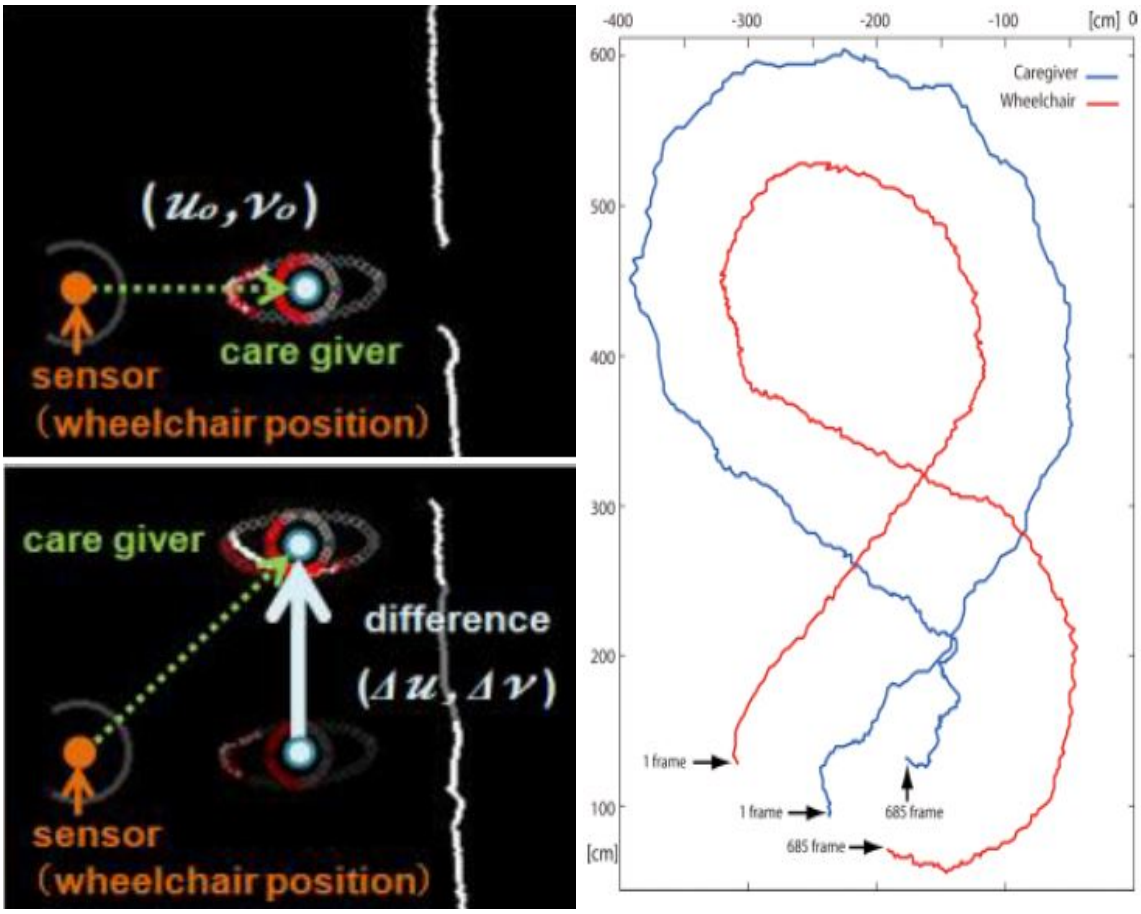

Figure 5.15: Trajectories of BMR and Companion

For body tracking with our system, we put a laser sensor at shoulder height on the wheelchair. Fig. 5.16 shows the companion following sensor arrangement and scanning position on the shoulder part. Our wheelchair follows the companion in side by side manner. Therefore, we divided the tracking areas into three section, 1) Forward zone 2) Stop and, 3) Backward zone. if the companion tracked the companion in either zone, our wheelchair acts accordingly. Moreover, while the wheelchair investigating the zone acts for mobilization, it will also calculate the body orientation for moving left or right direction. Fig. 5.17 illustrates the wheelchair navigation with the body orientation to the left or right. In the fig 5.18 shows the body tracking in the above mentioned three zones. Finally, we did some experiment with our new BMR incorporating the functionaries of companion following shows in Fig. 5.19.

Figure 5.16: Apparatus of companion following.

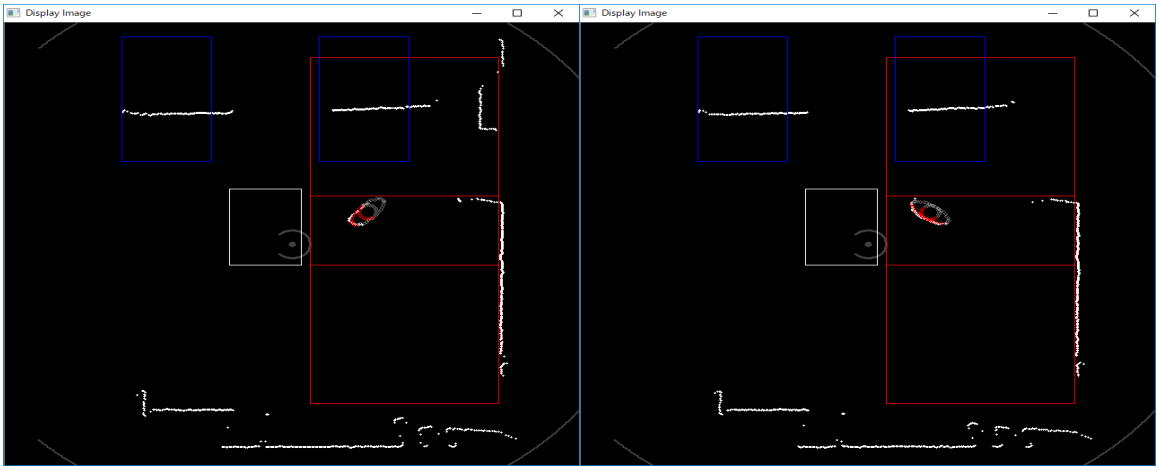

Body orientation LEFT Body orientation RIGHT

Figure 5.17: Apparatus of companion following.

Forward zone

Stop zone

Backward zone

Figure 5.18: Tracking the companion in three different zones.

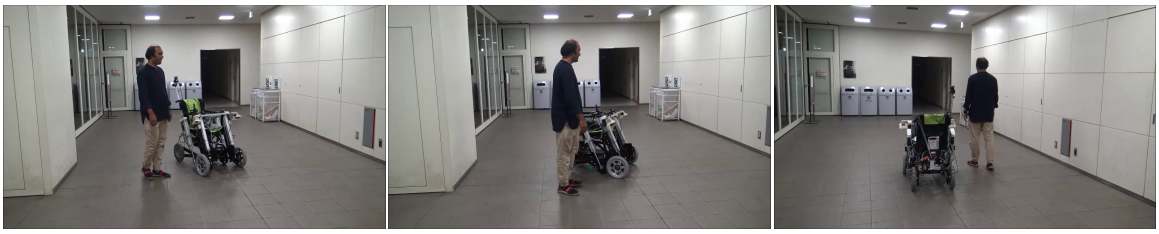

a) The wheelchair changing position according to body orientation

Forward zone Stop zone Backward zone

b) The wheelchair is navigating according to body position in zones

Figure 5.19: The wheelchair is navigating according to the body orientation and position.

5.8 Adjust Wheelchair Position

It is very important to consider the wheelchair position according to the bus door location for boarding. When our wheelchair detected the bus door position using our image recognition system, the wheelchair may stand on left side of the bus or right side of the bus. Therefore, the wheelchair needs to adjust its position to align itself straight to the door so that it can avoid collision with the door. In the previous section, we have discussed the sensor position in a wheelchair. Fig. 5.20 shows that our wheelchair can scan the bus body horizontally. In a particular frame, the position of the wheelchair is in the middle. We calculate the gravity position of the scan data from the left and right side of the bus body. Moreover, find the distance from each gravity point to the wheelchair. If the distance of the wheelchair from the left side of the bus body is larger than the right side, then wheelchair position is on the right of the bus. Similarly, If the distance of the wheelchair from the right side of the bus body is larger than the left side, then wheelchair position is on the left of the bus. Otherwise, the wheelchair is standing straight to the bus door. Fig. 5.21 shows the experiment result of our system which detects the wheelchair position.

Figure 5.20: Laser scanner data position on bus body.

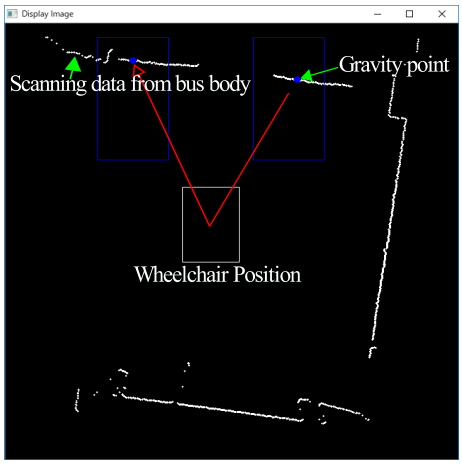

(a) The wheelchair is on right side of the bus

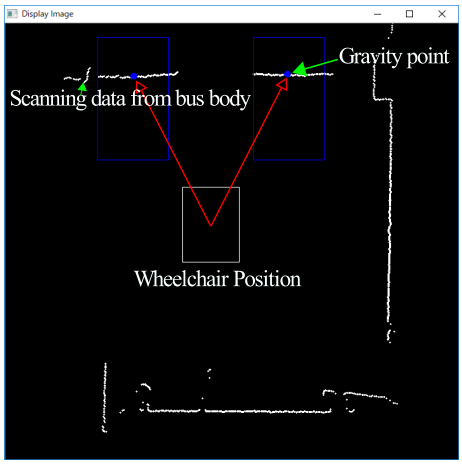

(b) The wheelchair is straight to the bus door

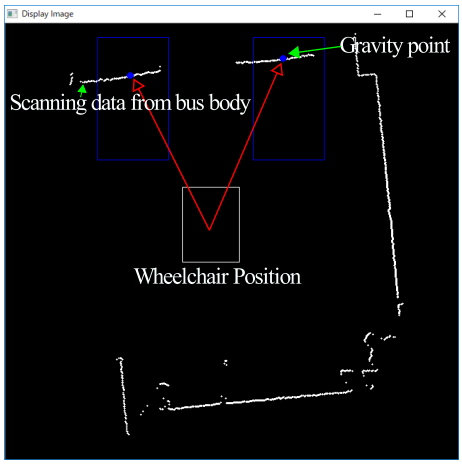

(c) The wheelchair is on left side of the bus

Figure 5.21: Laser scanner data position on bus body.

5.9 Chapter Summary

In this chapter, we introduce a new mechanism of sensing for getting the heights of bus doorsteps for autonomous bus boarding. Though our experiments were conducted in an indoor environment, we demonstrated successfully operation of the proposed system using our method for measuring the height of the bus doorstep. Moreover, the wheelchair plays a warning sound for its movements while its boarding to help other passenger cooperate with the wheelchair. According to our results in step detection and measurement, our system is able to detect the bus door and measure the approximate height of the doorstep, which grants freedom of movement to the wheelchair user. Moreover, we propose a companion following robotic wheelchair that can follow its companion for boarding and disembarking from buses. Additionally, it reduces the workload of the companion of the wheelchair user by helping in boarding and disembarking from the bus.

Our wheelchair has successfully demonstrated autonomous bus boarding in indoor mock-up and real bus experiment. Of course, real world scenarios are a bit different so in the future, we will conduct more experiments in real environments at bus stops and also identify moving objects with sensor data such as escalator steps. Thereby making it so the BMR could ride on escalators and increase its mobility.

Chapter 6

Conclusions and Future Works

6.1 Conclusions

This thesis presents an interdisciplinary research approach that combines techniques and methods from several research domain like sociology, psychology and human-robot interaction. Furthermore, it also presents an incremental studying and designing the methods to estimates human robot interaction for smooth navigation in urban environments. Additionally, it demonstrated and evaluated the effectiveness of the designed sensor system for robotic wheelchair to measure the height of any objects such as bus doorsteps and stairsteps.

The theoretical contributions of this work consist of a set of new knowledge of robot navigation in unknown environments to find objects using only laser sensors and help a deeper understanding on human-robot interaction. Our novel sensor framework can also derived a new era of 3D projection of the terrain condition while running.

Technical contribution of this thesis, we introduce a new mechanism of sensing for getting the heights of bus doorsteps for autonomous bus boarding. Though our experiments were conducted in a controlled outdoor environment, we demonstrated successfully operation of the proposed system using our method for measuring the height of the bus doorstep. Moreover, the wheelchair plays a warning sound for its movements while its boarding to help other passenger cooperate with the wheelchair. According to our results in step detection and measurement, our system is able to detect the bus door and measure the approximate height of the doorstep, which grants freedom of movement to the wheelchair user. Our wheelchair has successfully demonstrated autonomous bus boarding. Moreover, we also propose a companion following robotic wheelchair that can follow its companion for boarding and disembarking from buses. Additionally, it reduces the workload of the companion of the wheelchair user by helping in boarding and disembarking from the bus. Safety measures are also

incorporated to the system by using sound and laser data mapping on the camera image. Moreover, our system also has the capabilities to sense the environment to detect objects like people, buses, and other trained objects according to the system configuration so that the wheelchair user would be free to roam around the city independently and comfortably.

6.2 Future Work

In this thesis, attempts have been made to solve a highly complies and unconventional design problem in HRI-designing a human-robot interaction for navigating a wheelchair in urban environments.

- In general, we tested our proposed system model for a specific scenario like bus boarding and disembarking but our sensor system can be used to find out the objects heights and width to make a 3D model of it without any complex computation of object modeling.
- 3D terrain model can be possible using our sensing system. We use only the intensity values for terrain recognition but our sensing framework can be works for gathering 3D cloud points to model an object with minimum data.
- Controlled laboratory settings was used for our experiments of the wheelchair sensing system. To prove the current approaches will be effective beyond controlled settings, future work needs to also situate designed behaviors in different real world scenarios and contexts.
- In this thesis, the mobility of the wheelchair is considered for only bus boarding but in future it should be tested in other urban environments such as escalator, train boarding and disembarking, walkway identification and following the blind marks on the road to follow the marks to reach any goals.

Publications

Journals:

[1]. **S. Al Mamun**, A. Lam, Y. Kobayashi, Y. Kuno, "Single Laser Bidirectional Sensing for Robotic Wheelchair Step Detection and Measurement", Book chapter Intelligent Computing Methodologies of the series Lecture Notes in Computer Science, vol 10363, pp-37-47, 2017.
[2]. **S. Al Mamun**, R. Suzuki, A. Lam, Y. Kobayashi, Y. Kuno, "Terrain Recognition for Smart Wheelchair", Book chapter Intelligent Computing Methodologies Volume 9773 of the series Lecture Notes in Computer Science pp 461-470, 2016.

Others:

[3]. A. Sarowar, **S. Al Mamun**, H. Fukuda, A. Lam, Y. Kobayashi, Y. Kuno, "Smart Robotic Wheelchair for Bus Boarding Using CNN Combined with Hough Transforms", Book chapter Intelligent Computing Methodologies Volume 10956 of the series Lecture Notes in Computer Science pp 163-172, 2018.
[4]. **S. Al Mamun**, H. Fukuda, A. Lam, Y. Kobayashi, Y. Kuno, "Companion Following Robotic Wheelchair with Bus Boarding Capabilities", IEEE International Conference on Informatics, Electronics and Vision (ICIEV 2018), Japan. Got best paper award and will be published in IEEE express digital library
[5]. **S. Al Mamun**, H. Fukuda, A. Lam, Y. Kobayashi, Y. Kuno, "Autonomous Bus Boarding Robotic Wheelchair using Bidirectional Sensing Systems", 13th International symposium on Visual Computing (ISVC 2018), USA. Accepted and published in Springer Lecture Notes series.

Bibliography

[1] R. Bostelman and J. Albus. Sensor experiments to facilitate robot use in assistive environemnts. In *Int. Conf. on Pervasive Technologies Related to Assistive Environments*, 2008.

[2] S. Carbonara and C. Guaragnella. Efficient stairs detection algorithm Assisted navigation for vision impaired people. In *Proceedings of IEEE International Symposium on Innovations in Intelligent Systems and Applications (INISTA)*, pages 313–318, 2014.

[3] T. Carlson and Y. Demiris. Increasing robotic wheelchair safety with collaborative control: Evidence from secondary task experiments. In *Robotics and Automation (ICRA), 2010 IEEE International Conference on*, pages 5582–5587. IEEE, 2010.

[4] Power chair with tank chassis. Tc-mobility. *Feb. 2018. [Online]. Available: http://www.tankchair.com.*

[5] R. E. Cowan and et. al. Recent trends in assistive technology for mobility. *Journal of neuroengineering and rehabilitation*, 9(1):20, 2012.

[6] P. Crawley. The brains behind the electric wheelchair, one of canadas great artifacts. *On line. Descargado de http://www. theglobeandmail. com/report-on-business*, 2012.

[7] J. d. R. Millan. BMI: Lessons from tests with impaired users. In *in Proc. Int. Winter Workshop Brain-Comput. Interface*, page 1, 2014.

[8] R. Desmond, M. Dickerman, J. Fleming, D. Sinyukov, J. Schaufeld, and T. Padir. Development of modular sensors for semi-autonomous wheelchairs. In *in Proc. IEEE Int. Conf. Technol. Practical Robot Appl.*, pages 1–6, 2013.

[9] J. Dong, Q. Chen, S. Yan, and A. Yuille. Towards unified object detection and semantic segmentation. In *Springer Book Lecture Notes in Computer Science*, volume 8693, page 299314, 2014.

[10] L. Fehr, W.E. Langbein, and S. B. Skaar. Adequacy of power wheelchair control interfaces for persons with severe disabilities: A clinical survey. *Journal of rehabilitation research and development*, 37(3):353, 2000.

[11] L. Fehr, W.E. Langbein, and S.B. Skaar. Adequacy of power wheelchair control interfaces for persons with severe disabilities: a clin-ical survey. In *Journal of Rehabilitation Research and Development*, volume 37(3), pages 353–360, 2000.

[12] K. Fritsch. The neoliberal circulation of affects: Happiness, accessibility and the capacitation of disability as wheelchair. *Health, Culture and Society*, 5(1):135, 2013.

[13] T. Fujita and Y. Kondo. Robot Arms. In *Book edited by Satoru Goto, ISBN 978-953-307-160-2*, 2011.

[14] T. Gomi and A. Griffith. Developing intelligent wheelchairs for the handicapped. In *Assistive Technology and Artificial Intelligence*, pages 150–178. Springer, 1998.

[15] M. Hamedi and et al. Comparison of different time-domain feature extraction methods on facial gestures. In *EMGs." Electromagnetics research symposium proceedings, KL. PIER*, 2012.

[16] S. Hemachandra, T. Kollarand N. Roy, and S. Teller. Following and interpreting narrated guided tours. In *Int. Conf. on Robotics and Automation (ICRA)*, 2011.

[17] C. W. Hsiao, Y. H. Chien, W. Y. Wang, I. H. Li, M. C. Chen, and S. F. Su. Wall following and continuously stair climbing systems for a tracked robot. In *IEEE 12th International Conference on Networking, Sensing and Control*, pages 371–375, 2015.

[18] Y. Hwang and J. Lee. Robust 3D map building for a mobile robot moving on the floor. In *IEEE International Conference on Advanced Intelligent Mechatronics (AIM)*, 2015.

[19] L.I. Iezzoni, E. P. McCarthy, R. B. Davis, and H. Siebens. Mobility difficulties are not only a problem of old age. *Journal of general internal medicine*, 16(4):235–243, 2001.

[20] Ability in Motion. Standing wheelchair. *Feb. 2018. [Online]. Available: http://abilityinmotion .com.au/products/standing-wheelchairs/.*

[21] M. Ishikawa and et al. Travel Device. volume Patent Number: WO2016/006248 A1, 2016.

[22] T. Iwase, R. Zhang, and Y. Kuno. Robotic Wheelchair Moving with the Caregiver. In *Proc. SICE-ICASE International Joint Conference 2006*, pages 238–243, 2006.

[23] S. Jain and B. Argall. Automated perception of safe docking locations with alignment information for assistive wheelchairs. In *in Proc. IEEE/RSJ Int. Conf. Intell. Robots Syst*, pages 4997–5002, 2014.

[24] Toyota Motor East Japan. Patrafour. *Feb. 2018. [Online]. Available: http://www.toyota-ej.co.jp/english/products/patrafour.html.*

[25] C. L Jones, J.M. Kosco, and M.A. Goodell. Power supply assembly for motorized vehicles, October 7 2008. US Patent 7,431,109.

[26] M. S. Kaiser, Z.I. Chowdhury, S. A. Mamun, A. Hussain, and M. Mahmud. A Neuro-Fuzzy Control System Based on Feature Extraction of Surface Electromyogram Signal for Solar-powered Wheelchair. In *Journal of Cognitive Computation*, volume 8-1, pages 1–9, 2016.

[27] Y. Kobayashi, Y. Kinpara, Takano, Y. Kuno, K. Yamazaki, and A. Yamazaki. Robotic wheelchair moving with caregiver collaboratively. In *In: Huang, D.-S., Gan, Y., Gupta, P., Gromiha, M.M. (eds.) ICIC 2011. LNCS (LNAI)*, volume 6839, page 523532, 2012.

[28] Y. Kuno, N. Shimada, and Y. Shirai. Look Where Youre Going: A Robotic Wheelchair Based on the Integration of Human and Environmental Observations. In *IEEE Robotics and Automation2003*, volume 10, pages 26–34, 2003.

[29] A. Lankenau and T. Rfer. A versatile and safe mobility assistant. *IEEE Robot Autom Mag*, 8 (1):29–37, 2001.

[30] F. Leishman, O. Horn V. Monfort and, and G. Bourhis. Driving assistance by deictic control for a smart wheelchair: The assessment issue. In *IEEE Trans. Human-Mach. Syst.,*, volume 44, pages 66–77, 2014.

[31] S. P. Levine, D. A. Bell, A. David, and Y. Koren. Navchair: An example of a shared-control system for assistive technologies. In *International Conference on Computers for Handicapped Persons*, pages 136–143. Springer, 1994.

[32] W. Liu and et al. SSD: Single Shot Multibox Detector. In *Proceedings of 14th European Conference on Computer Vision*, volume 9905, pages 21–37, 2016.

[33] J. Lv and et al. Indoor slope and edge detection by using two-dimensional EKF-SLAM with orthogonal as-sumption. In *International Journal of Advanced Robotic Systems (2015)*, 2015.

[34] J. Lv, Y. Kobayashi, Y. Hoshino, and T. Emaru. Slope detection based on Orthogonal Assumption. In *IEEE/SICE International Symposium on system Integration (SII)*, 2012.

[35] S. A. Mamun, A. Lam, Y. Kobayashi, and Y. Kuno. Single Laser Bidirectional Sensing for Robotic Wheelchair Step Detection and Measurement. In *Springer Lecture Notes in Computer Science Intelligent Computing Methodologies*, volume 10363, pages 37–47, 2017.

[36] S. A. Mamun, R. Suzuki, A. Lam, Y. Kobayashi, and Y. Kuno. Terrain Recognition for Smart Wheelchair. In *chapter Intelligent Computing Methodologies, the series Lecture Notes in Computer Science*, volume 9773, pages 461–470, 2016.

[37] S.A. Mamun, M.S. kaiser, M.R. Ahmed, M.S. Islam, and M.I. Islam. Performance Analysis of Optical Wireless Communication System Employing Neuro-Fuzzy Based Spot-diffusing Techniques. In *Journal of Communication and Networks*, volume 5, pages 260–265, 2013.

[38] O. Mazumder, A. S. Kundu, R. Chattaraj, and S. Bhaumik. Holonomic wheelchair control using EMG signal and joystick interface. In *in Proc. Recent Adv. Eng. Comput. Sci*, pages 1–6, 2014.

[39] A. R. Meyers, J. J. Anderson, D. R. Miller, K. Schipp, and H. Hoenig. Barriers, facilitators, and access for wheelchair users: sbstantive and methodologic lessons from a pilot study of environmental effects. In *Social Science and Medicine*, volume 55, pages 1435–1446, 2002.

[40] J. Min, K. Lee, S. Lim, and D. Kwon. Human Friendly Interfaces of Wheelchair Robotic System for Handicapped Persons. In *Proc. International Conference on Intelligent Robots and Systems (IROS)*, volume 2, pages 1505–1510, 2011.

[41] C. Montella, M. Pollock, D. Schwesinger, and J. Spletzer. Stochastic classification of urban terrain for smart wheelchair navigation. In *Proceedings of the IROS Workshop on Progress, Challenges and Future Perspectives in Navigation and Manipulation Assistance for Robotic Wheelchairs*, 2012.

[42] I. Moon, M. Lee, J. Ryu, and M. Mun. Intelligent robotic wheelchair with emg-, gesture-, and voice-based interfaces. In *Intelligent Robots and Systems, 2003.(IROS 2003). Proceedings. 2003 IEEE/RSJ International Conference on*, volume 4, pages 3453–3458. IEEE, 2003.

[43] Munoz, R. Rong, X. Tian, and Yingli. Depth-aware indoor staircase detection and recognition for the visually impaired. In *Multimedia & Expo Workshops (ICMEW), 2016 IEEE International Conference on*, pages 1–6. IEEE, 2016.

[44] Z. Nemoto, H. Takemura, and H. Mizoguchi. Development of Small-sized Omnidirectional Laser Range Scanner and Its Application to 3D Background Difference. In *Proceedings of IEEE 33rd Annual Conference Industrial Electronics Society(IECON 2007)*, page 22842289, 2007.

[45] S. Obwald, A. Grg, A. Hornung, and M. Bennewitz. Autonomous climbing of spiral staircases with humanoids. In *Proc. of the IEEE/RSJ Int. Conf. on Intelligent Robots and Systems (IROS)*, 2011.

[46] S. P. Parikh, V. Grassi, V. Kumar, and Jr. J. Okamoto. Usability study of a control framework for an intelligent wheelchair. In *Robotics and Automation, 2005. ICRA 2005. Proceedings of the 2005 IEEE International Conference on*, pages 4745–4750. IEEE, 2005.

[47] S. P. Parikh, R. Rao, S. Jung, V. Kumar, J. P. Ostrowski, and C.J. Taylor. Human robot interaction and usability studies for a smart wheelchair. In *Intelligent Robots and Systems, 2003.(IROS 2003). Proceedings. 2003 IEEE/RSJ International Conference on*, volume 4, pages 3206–3211. IEEE, 2003.

[48] F. Pasteau, A. Krupa, , and M. Babel. Vision-based assistance for wheelchair navigation along corridors. In *Proc. IEEE Int. Conf. Robotic Automation*, page 44304435, 2014.

[49] J. Pineau, R. West, A. Atrash, J. Villemure, and F. Routhier. On the feasibility of using a standardized test for evaluating a speech-controlled smart wheelchair.

In *International Journal of Intelligent Control System*, volume 16 (2), pages 124–131, 2011.

[50] J. Poppinga, A. Birk, and K. Pathak. Hough based terrain classification for real time detection of drivable ground. In *Journal of Field Robotics*, volume 25 No. 1-2, page 6788, 2008.

[51] G. Quaglia, W. Franco, and R. Oderio. Wheelchair. q, a motorized wheelchair with stair climbing ability. *Mechanism and Machine Theory*, 46(11):1601–1609, 2011.

[52] W.M. Rand. Objective criteria for the evaluation of clustering methods. In *Journal of American Statistical Association*, volume 66, pages 846–50, 1971.

[53] D.K. Rathore, P. Srivastava, S. Pandey, , and S. Jaiswal. A novel multipurpose smart wheelchair. In *in Proc. IEEE Students Conf. Elect., Electron. Comput. Sci.*, pages 1–4, 2014.

[54] J. Redmon and et al. You only look once: Unified real-time object detection. In *Proceedings of the IEEE Conference on Computer Vision and Pattern Recognition*, pages 779–788, 2016.

[55] L. P. Reis, R. Braga, M. Sousa, and A.M. Moreira. Intellwheels mmi: A flexible interface for an intelligent wheelchair. In *Robot Soccer World Cup*, pages 296–307. Springer, 2009.

[56] Y. Satoh and K. Sakaue. An Omnidirectional Stereo Vision-Based Smart Wheelchair. In *Journal on Image and Video Processing*, volume 87646, 2007.

[57] T. Schwarze and Z. Zhong. Stair detection and tracking from egocentric stereo vision. In *IEEE International Conference on Image Processing (ICIP)*, pages 2690–2694, 2015.

[58] D. Schwesinger, A. Shariati, C. Montella, and J. Spletzer. A smart wheelchair ecosystem for autonomous navigation in urban environments. *Autonomous Robots*, 41(3):519–538, 2017.

[59] R. Sheh, M. Kadous, C. Sammut, , and B. Hengst. Extracting terrain features from range images for autonomous random step field traversal. In *Proceedings of IEEE International Workshop on Safety, Security and Rescue Robotics*, 2007.

[60] R. Sheh, M. Kadousand C. Sammut, and B. Hengst. Extracting terrain features from range images for autonomous random step field traversal. In *Proceedings of IEEE International Workshop on Safety, Security and Rescue Robotics*, 2007.

[61] J. Shen, B. Xu, M. Pei, and Y. Jia. A low-cost tele-presence wheelchair system. In *IEEE/RSJ International Conference on Intelligent Robots and Systems (IROS)*, pages 2452–2457, 2016.

[62] Y. Shin, J. Park, J. Bae, and M. Baeg. A Study on Reliability Enhancement for Laser and Camera Calibration. In *International Journal of Control, Automation, and Systems.*, volume 10(1), pages 109–116, 2012.

[63] R. Simpson. Smart Wheelchair Component System. In *Journal of Rehabilitation Res. Development*, volume 41 (3B), pages 429–442, 2004.

[64] D. Sinyukov, R. Desmond, M. Dickerman, J. Fleming, J. Schaufeld, and T. Padir. Multi-modal control framework for a semi-autonomous wheelchair using modular sensor designs. In *Intell. Serv. Robot*, volume 7 (3), page 145155, 2014.

[65] R. Suzuki, T. Yamada, M. Arai, Y. Sato, Y. Kobayashi, and Y. Kuno. Multiple robotic wheelchair system considering group communication. In *International Conference on Visual Computing(ISVC2014)*, volume 8887, pages 805–814, 2014.

[66] All terrain wheelchair. Observer-mobility. *Feb. 2018. [Online]. Available: http://www.observer-mobility.com.*

[67] A. Voulodimos, N. Doulamis, A. Doulamis, and E. Protopapadakis. Deep Learning for Computer Vision: A Brief Review. In *Journal of Computational Intelligence and Neuroscience*, volume 2018, page 13, 2018.

[68] L. Wan and E. Tam. Power wheelchair assessment and training for people with motor impairment. 2010.

[69] Worldvank Report. Overview of Disability. In *http://www.worldbank.org/en/topic/disability/overview*, volume September 21, 2016, Access date- 22 February, 2016.

[70] J. Xu, G. Grindle, B. Salatin, D. Ding, and R. A. Cooper. Manipulability evaluation of the personal mobility and manipulation appliance (permma). In *Int. Symp. on Quality of Life Technology*, 2009.

[71] T. Yamada, T. Ito, and A. Ohya. Detection of road surface damage using mobile robot equipped with 2D laser scan-ner. In *IEEE/SICE International Symposium on. System Integration (SII), 2013*, 2013.

[72] U. Yayan, B. Akar, F. Inan, , and A. Yazici. Development of indoor navigation software for intelligent wheelchair. In *in Proc. IEEE Int. Symp. Innovations Intell. Syst. Appl. Proc*, pages 325–329, 2014.

[73] C. Yi, S. Jeong, and J. Cho. Map Representation for Robots. In *Smart Computing Review*, volume 2(1), 2012.

[74] J. D. Yoder, E.T. Baumgartner, and S. B. Skaar. Initial results in the development of a guidance system for a powered wheelchair. *IEEE Transactions on Rehabilitation Engineering*, 4(3):143–151, 1996.